Check for updates

Received: 30 June 2020 | Revised: 27 November 2020 | Accepted: 28 November 2020

DOI: 10.1111/pce.13972

ORIGINAL ARTICLE

Plant, Cell & Environment WILEY

Transcriptome and translatome changes in germinated pollen under heat stress uncover roles of transporter genes involved in pollen tube growth

Laetitia Poidevin[1] | Javier Forment[1] | Dilek Unal[2] | Alejandro Ferrando[1]

[1]Instituto de Biología Molecular y Celular de Plantas, Consejo Superior de Investigaciones Científicas-Universitat Politècnica de València, Valencia, Spain

[2]Biotechnology Application and Research Center, and Department of Molecular Biology, Faculty of Science and Letter, Bilecik Seyh Edebali University, Bilecik, Turkey

Correspondence
Alejandro Ferrando, Instituto de Biología Molecular y Celular de Plantas, Consejo Superior de Investigaciones Científicas-Universitat Politècnica de València, Valencia, Spain.
Email: aferrando@ibmcp.upv.es

Funding information
Ministerio de Ciencia e Innovación, Grant/Award Number: BIO2015-70483-R

Abstract

Plant reproduction is one key biological process that is very sensitive to heat stress and, as a result, enhanced global warming becomes a serious threat to agriculture. In this work, we have studied the effects of heat on germinated pollen of *Arabidopsis thaliana* both at the transcriptional and translational level. We have used a high-resolution ribosome profiling technology to provide a comprehensive study of the transcriptome and the translatome of germinated pollen at permissive and restrictive temperatures. We have found significant down-regulation of key membrane transporters required for pollen tube growth by heat, thus uncovering heat-sensitive targets. A subset of the heat-repressed transporters showed coordinated up-regulation with canonical heat-shock genes at permissive conditions. We also found specific regulations at the translational level and we have uncovered the presence of ribosomes on sequences annotated as non-coding. Our results demonstrate that heat impacts mostly on membrane transporters thus explaining the deleterious effects of heat stress on pollen growth. The specific regulations at the translational level and the presence of ribosomes on non-coding RNAs highlights novel regulatory aspects on plant fertilization.

1 | INTRODUCTION

The evidence of a rapid global warming since the beginning of the industrial epoch is very solid (Intergovernmental Panel on Climate Change, 2014) and its global impact seems to have an anthropogenic origin, as paleoclimate reconstructions found no evidence of world-wide coherent warm or cold periods in the preindustrial times (Neukom, Steiger, Gómez-Navarro, Wang, & Werner, 2019). According to the known drivers of climate change, global warming predictions have been made with pessimistic scenarios especially for agriculture in low latitudes (Rosenzweig et al., 2014). The negative impact of enhanced global warming on agriculture poses serious risks for future food security and demands smart food system management strategies (Vermeulen, Campbell, & Ingram, 2012). Under this scenario, understanding how increased temperature impacts plant biology is an important task.

Plant reproduction is considered the most sensitive stage of plant development by the effects of global warming (Hedhly, Hormaza, & Herrero, 2009) and, for many crop plants, pollen seems to be particularly vulnerable to high temperatures (Herrero & Johnson, 1980; Ledesma & Sugiyama, 2005; Sato, Peet, & Thomas, 2002; Zinn, Tunc-Ozdemir, & Harper, 2010). Pollen sensitivity to heat occurs not only throughout its development prior to anther dehiscence but also during germination and pollen tube growth (Kakani et al., 2005; Kakani, Prasad, Craufurd, & Wheeler, 2002). Upon landing on the stigmatic tissue of the pistil, pollen grains of flowering plants hydrate and germinate to immediately initiate pollen tube growth over long distances to deliver the male gametes to the egg and central cells in the embryo sac for the double fertilization process (Lord & Russell, 2002). Growth of the pollen tube from the stigma to the ovules occurs at extremely rapid rates and requires a fine regulation of subcellular processes such as: well-ordered vesicle transport, precise cytoskeleton arrangements,

 © 2020 John Wiley & Sons Ltd.

strict and local pH establishment, proper energy management with amyloplast and mitochondrial logistics and delicate regulation of regulatory ion fluxes for osmotic adjustment (K^+ transport) and signalling (Ca^{2+} transport). This impressive machinery demands exquisite coordination among all these processes for the rapid transport of germinal sperm cells to the micropyle (Chebli, Kroeger, & Geitmann, 2013; Hepler, Rounds, & Winship, 2013; Michard, Simon, Tavares, Wudick, & Feijó, 2017). One important aspect of this optimized cellular growth is the presence of local pH gradients with an acidic apex region and an alkaline band in the clear zone followed by a subapical region of acidic pH (Feijó, Sainhas, Hackett, Kunkel, & Hepler, 1999; Hepler & Winship, 2015). This complex organization of events demands an optimized protein synthesis machinery (Cheung & Wu, 2007). Ultrastructural analysis of pollen tube growth at high temperature revealed alterations in rough-endoplasmic reticulum, Golgi apparatus and mitochondria (Kandasamy & Kristen, 1989), thus supporting the notion that protein translation, vesicle transport and energy depletion during pollen tube growth may be limiting steps in the adaptation to high-temperature conditions. Molecular studies have uncovered heat responses in pollen subjected to high temperature similar to other plant cell types (Rieu, Twell, & Firon, 2017). In addition, several "omics" studies have been performed to characterize the response of pollen under heat stress conditions (Begcy et al., 2019; Chaturvedi, Ischebeck, Egelhofer, Lichtscheidl, & Weckwerth, 2013; Jegadeesan et al., 2018; Keller et al., 2018). To complement these approaches, the use of next generation sequencing of nucleic acids (NGS) techniques (Reuter, Spacek, & Snyder, 2015), is expected to help gain deeper insight in the response of pollen to heat stress conditions.

A breakthrough in the studies of mRNA translation was achieved with the development of the ribosome profiling technique (also called Ribosome Footprinting, Riboprofiling or Ribo-Seq), a ribosome-centric approach to isolate and sequence ribosome-protected mRNA fragments (RPFs) after RNase treatment that provides a quantitative profile of translation across the transcriptome with sub-codon resolution (Ingolia, Ghaemmaghami, Newman, & Weissman, 2009). The advantage of Riboprofiling is that, in parallel with massive sequencing of ribosome footprints, total RNA is also subjected to high-throughput sequencing thus allowing the direct comparison of the transcriptome, the translatome and the calculations of translational efficiencies for the complete set of transcripts (Ingolia, 2016).

Here we have used Riboprofiling with Arabidopsis pollen germinated *in vitro* under both optimum and high-temperature conditions. We provide high-resolution transcriptome and translatome profiles of pollen tubes germinated at basal temperature, and show their changes in response to heat stress. We have found that *in vitro* germinated pollen responds to high temperature by up-regulating heat shock genes in a similar manner to the vegetative organs. Heat stress also down-regulated specifically many membrane transporters, including K^+ and carbohydrate co-transporters, thus finding a suitable explanation to the deleterious effects of high temperature on pollination. A subset of these transporters is up-regulated during *semi in vivo* pollen development, when heat shock genes are also expressed, illustrating the importance of these heat-sensitive functions during plant fertilization. Moreover, we have found specific regulations at the translational level and the unexpected presence of ribosome footprints on non-coding RNAs. Thus, our analysis of combined transcriptome and translatome is revealing novel insights on pollen responses to heat stress, including a tight connection between heat shock gene expression and membrane transporters that promote pollen tube growth and male fertility.

2 | MATERIALS AND METHODS

2.1 | Large-scale pollen collection using vacuum filtration

About 20.000 *A. thaliana* (Col-0) plants were grown in greenhouse for 4 weeks in a mixture of 25% vermiculite, 25% perlite and 50% soil under long-day photoperiod cycles. Pollen collection was performed by vacuum filtration following described protocols (Johnson-Brousseau & McCormick, 2004). Pollen was then scrapped off the 6 μm nylon mesh, and dried overnight under a chemical hood in a 2 mL tube. After weighing, a silica bead was added to the pollen and the samples were placed at −20°C. Harvests were done every second day for about 2 weeks. Yields ranged from 10 to 55 mg of pollen per day. A small aliquot from each sample was kept in a second tube for pollen viability and contamination assays. The evaluation of contamination was performed by microscopic examination of the samples, where both bacteria and fungi are readily visible. The whole experiment was repeated 3 times to obtain 3 biological replicates.

2.2 | Pollen growth assays

The pollen tube growth was assayed using published protocols (Boavida & McCormick, 2007). Three- to six-month-old frozen pollen grains were first rehydrated for 1 h in a humid chamber. Pollen was then germinated on an agar medium containing 10% sucrose, 0.01% boric acid, 1 mM $MgSO_4$, 5 mM $CaCl_2$, 5 mM KCl and 1.5% low-melting agarose, pH 7.5 (adjusted with 0.1 M NaOH). For microscopic pollen examination, 1 mL of melted germination medium was spread on a glass microscope slide to build a flat pad where pollen can be spread after the agarose is solidified. The slides were placed inside a moisture incubation chamber to avoid dehydration of the medium, and incubated in the dark at 24°C or 35°C, for the indicated time. Pictures were taken with a Leica DM5000 microscope. Quantifications of pollen germination and tube length were performed with the IMAGEJ Software (Schindelin et al., 2012) using the cell counter and NeuronJ plug-ins (Meijering et al., 2004). Germinated pollen was scored positively for grains with a pollen tube length of at least the pollen diameter. For the Riboprofiling experiments, the protocol was scaled up to 10 cm-square petri dishes containing 30 mL of pollen germination medium. 25 mg of pollen grains were spread per plate with a soft brush in a moisture incubation chamber, sealed, and placed in the dark at 24°C or 35°C for 5 h before being collected. Three

13653040, 2021, 7, Downloaded from https://onlinelibrary.wiley.com/doi/10.1111/pce.13972 by Bilecik Seyh Edebali, Wiley Online Library on [17/12/2025]. See the Terms and Conditions (https://onlinelibrary.wiley.com/terms-and-conditions) on Wiley Online Library for rules of use; OA articles are governed by the applicable Creative Commons License

plates per temperature were prepared from each of the biological replicates. For the RTqPCR experiments the protocol was the same, with two biological replicates of 6 month-old frozen pollen grown for 5 h at 24°C or 35°C, and one additional treatment for 3 h at 24°C and two additional hours at 35°C.

2.3 | Preparation of RNA and RPF libraries for Riboprofiling

Pollen was scrapped from the plates and ground in liquid nitrogen in an optimized ice-cold extraction buffer for Riboprofiling experiments (Hsu et al., 2016) containing: 0.1% Tris–HCl pH 8, 1% sodium deoxycholate, 40 mM KCl, 20 mM $MgCl_2$, 10% polyoxyethylene-10-tridecyl ether, 1 mM DTT,100 μg/mL cycloheximide, 10 U/mL DNAse I (Illumina, USA). After centrifugation, the supernatants were transferred into a pre-chilled tube and split into 100 μL (for RNA library) and 200 μL (for RPF library) aliquots. Estimation of RNA concentration was performed with NanoDrop ND1000 (Thermo Fisher Scientific, USA). The libraries were obtained using the Illumina® TruSeq® Ribo Profile Mammalian kit (Illumina), with slight modifications to the standard protocol. The 100 μL samples of total RNA were denatured by adding SDS to 1% final concentration and kept aside until needed. In parallel, generation of ribosome protected fragment consisted of digesting 200 μg of RNA with 100 U of TruSeq Ribo Profile Nuclease for 1 h at 21°C, with shaking at 300 rpm. Reaction was stopped by adding 1 U/μL of SUPERase In RNase Inhibitor (Thermo Fisher Scientific, USA), then ribosomes were purified by size exclusion columns using MicroSpin S-400 columns following provider's recommendations (GE Healthcare, UK). Recovered ribosomes were denatured by adding SDS to 1% final concentration, and then both ribosome-bound RNA and denatured total RNA samples were purified with RNA Clean & concentrator-25 kit (Zymo Research, USA). RPFs were size-fractionated on 15% urea polyacrylamide gel electrophoresis (PAGE), by recovering fragments of 28 to 30 nt after gel staining with SYBR Gold (Thermo Fisher Scientific, USA), using Truseq Ribo Profile RNA Control as reference. Purified RPFs and total RNAs were rRNA depleted using the Ribo-Zero Magnetic bead kit (Illumina, USA) by adding 50 μL or 100 μL of magnetic beads per RPF or RNA samples respectively, according to manufacturer's instructions. Heat fragmentation of total RNA, end repair of RNA and RPF as well as downstream steps for 3′ adapter ligation, adaptor removal, reverse transcription, PAGE purification of cDNA and cDNA circularization were done following strictly the Illumina kit protocol. The cDNA Libraries were amplified by 13 and 15 PCR cycles for RNA and RPF, respectively. Library fragments of expected size were purified by non-denaturing PAGE and, after purification, DNA integrity and concentration were checked using Bioanalyzer 2100 expert High Sensitivity DNA Assay (Agilent Technologies, Inc). Equimolar (5 nM) pools of libraries were prepared for 100 bp paired-end sequencing on Illumina HiSeq4000 platform at Macrogen (Korea). Raw sequences and table containing counts and normalized TPM values generated in this study have been deposited in the Gene Expression Omnibus database (http://www.ncbi.nlm.nih.gov/geo/) with the accession number GSE145795.

2.4 | RTqPCR analsysis

The protocol for RNA extraction was the same as for the RNA sequencing libraries until the step of RNA purification with RNA Clean & concentrator-25 kit (Zymo Research, USA). After the estimation of RNA concentration performed with NanoDrop ND1000 (Thermo Fisher Scientific, USA), 500 ng of total RNA were used for cDNA synthesis with the PrimeScript RT reagent kit (Takara Bio Inc. Otsu, Shiga, Japan) in a volume of 10 μL and finally diluted with sterile water to 50 μL. Real time PCR was performed in triplicates with 0.5 μL of the cDNA using the PyroTaqEvaGreen qPCR mix according to the manufacturer's instructions (Cultek Molecular Bioline, Spain). The primers used are shown in Table S7 with the indicated references (Chen & Brandizzi, 2012; Czechowski, Stitt, Altmann, Udvardi, & Scheible, 2005; Ohama et al., 2016; Sze et al., 2004). The housekeeping gene (YSL8) suggested in previous studies as normalization gene (Czechowski et al., 2005) was analysed in our RNA sequencing libraries to confirm stable expression in pollen at different temperatures. Primers designed in this study were designed with the web tool pcrEfficiency (Mallona, Weiss, & Egea-Cortines, 2011). The quantification and statistical analysis of relative mRNA expression was performed as described (Ahmed & Kim, 2018).

2.5 | Bioinformatic data analysis

To determine which of the paired files corresponded to reads from the coding strand, htseq-count v0.10 was used and the files were kept for downstream analysis. After quality analysis with FastQC v0.11.5, reads were processed for adaptor and low quality regions removal with cutadapt v1.16 (Martin, 2011). Clean, trimmed reads ranging between 20 to 40 nt for RNA samples and 20 to 30 nt for RPF samples were selected for downstream analysis. Reads corresponding to rRNA, tRNA, snRNA and snoRNA sequences were identified and removed with bowtie2 v2.3.2 (Langmead & Salzberg, 2012) using the set of rRNA, tRNA, snRNA and snoRNA TAIR10 sequences downloaded from Ensembl Plants (Cunningham et al., 2018). The remaining reads were mapped to the TAIR10 Arabidopsis reference genome using HISAT2 v2.1.0 (Kim, Paggi, Park, Bennett, & Salzberg, 2019), and entries for reads mapping to more than one locus were excluded with samtools v1.5 (H. Li et al., 2009). For RPF samples, 27 to 28 nt uniquely mapped reads were selected for downstream analysis using the Linux command line "awk." The final sets of RNA 20 to 40 nt and RPF 27 to 28 nt uniquely mapped reads were assigned to specific genes, 5′UTRs, CDSs and 3′UTRs using htseq-count v0.10 (Anders, Pyl, & Huber, 2014) and the last Arabidopsis TAIR10 genome annotation from Araport11 (Cheng et al., 2017) containing 37,336 genes. Correlation heat-maps were obtained with multiBamSummary and plotCorrelation, from the deepTools v3.1.0 package (Ramírez

13653040, 2021, 7, Downloaded from https://onlinelibrary.wiley.com/doi/10.1111/pce.13972 by Bilecik Seyh Edebali, Wiley Online Library on [17/12/2025]. See the Terms and Conditions (https://onlinelibrary.wiley.com/terms-and-conditions) on Wiley Online Library for rules of use; OA articles are governed by the applicable Creative Commons License

et al., 2016). PCA analysis was performed in R v3.4.4, using the cluster v2.1.0 (Mächler, Rousseeuw, Struyf, Hubert, & Hornik, 2012), Biobase v2.38.0 (Huber et al., 2015), qvalue v2.10.0 (Storey, Bass, Dabney, & Robinson, 2019) and fastcluster v1.1.25 (Müllner, 2013) packages. Ribowave v1.0 (Xu et al., 2018) was used for the study of periodicity of RPF reads, and Xtail v1.1.5 (Xiao, Zou, Liu, & Yang, 2016) for the differential transcriptional/translational analysis and for the studies of differential translational efficiency. The fold change comparisons always refer to the 35°C data (treatment) versus the 24°C data (no treatment). The GO term enrichment analysis was performed using the web-based g:Profiler toolset (Raudvere et al., 2019) with the g:SCS threshold method and either annotated genes or custom list of genes when indicated. RStudio v1.2.5001 (TeamRStudio, 2019) was used with the ggplot2 library for correlation plots and periodicity graphs, and with the UpSetR library for the intersection set analysis. To obtain the heat-map viewer for gene expression under different pollen developmental stages we used the web-based tool "Arabidopsis Heat Tree Viewer" (http://arabidopsis-heat-tree.org/). Comparison of gene lists with Venn diagrams was performed with the web tool Venny 2.1 (Oliveros, 2015). Graphical visualization of the read coverage on mapped genes was performed with the Integrative Genomics Viewer (IGV) (Robinson et al., 2011).

3 | RESULTS

3.1 | Establishing the protocol for Riboprofiling studies of pollen response to elevated temperature

We first established a protocol for large-scale pollen collection and *in vitro* pollen germination necessary to perform the Riboprofiling studies. We grew around 60,000 *A. thaliana* Col-0 plants under greenhouse conditions to collect pollen by vacuum filtration with a modified vacuum cleaner as previously published (Johnson-Brousseau & McCormick, 2004). Pollen was collected and, after dehydration, stored in dry aliquots at −20°C to allow the synchronous processing of the samples. A small amount of every frozen aliquot, after proper rehydration, was tested for germination under *in vitro* conditions. Only non-contaminated samples showing similar pollen germination percentages were used to quantify germination and pollen tube growth under optimum temperature at 24°C and limiting high-temperature conditions. The effects of the high temperature on pollen growth have not been so well characterized for *A. thaliana* pollen germinated *in vitro*, so we performed preliminary tests in the range 32°C to 35°C and found that treatments at 35°C restricted pollen germination and growth without complete inhibition. Therefore we used 35°C as the limiting high-temperature condition. As shown in Figure 1A (left), large variations in pollen germination rates after cold-storage were found as it was shown in previous studies (Bou Daher, Chebli, & Geitmann, 2009) with a maximum germination percentage after 5 h of incubation at both temperatures, and germination was slightly affected by the elevated temperature. The pollen tube growth displayed more reproducible patterns allowing us to measure significant differences between both temperatures, showing a severe growth inhibition at 35°C from early growth stages (Figure 1A, right). We, therefore, selected a time point of 5 h of incubation to collect three biological replicates of germinated pollen both at 24°C and 35°C for Riboprofiling analysis. Once *in vitro* germinated pollen was collected by scrapping from the plates, every replicate was divided in two samples for parallel isolation of total RNA (RNAs) and ribosome protected fragments (RPFs), therefore, a total of 12 libraries were prepared for next-generation sequencing (Figure 1B).

3.2 | Riboprofiling shows enrichment of coding sequences in germinated pollen

High-throughput sequencing was performed using Illumina HiSeq4000, yielding a total of over 3,100 million paired-end 100 base reads for the 12 libraries. The correlation and PCA analyses among the different RNA and RPF libraries are shown in Figure S1. The data show very good cluster separations between the type of library (RNA and RPF) and between the temperature treatments (24°C and 35°C), with correlation coefficients above 0.95 among the triplicates. We then analysed the RNA and the RPF read length distributions (Figure S2A). Although RNA reads were spread in a large range size from 20 to 40 nucleotides, the RPFs showed a notable accumulation around 27 and 28 nucleotides as expected for ribosome footprint protection in *A. thaliana* (Hsu et al., 2016). After mapping to the *A. thaliana* reference genome, the read distributions were computed on 5′UTR, coding regions and 3′UTR, showing that ribosome footprints mapped to higher extent to coding sequences and to lesser extent to untranslated regions compared to RNA reads (Figure S2B). The bias of RPFs towards the translated frame can be used to infer the position of the ribosomal peptidyl-site (P-site) as a very good proxy to determine whether the ribosome is in frame with either start or stop codons. As an example, the meta-gene computing analysis of RPF distribution for 28 nucleotide fragments of one library is shown in Figure S2C,D. The data clearly show a well-defined trinucleotide (3-nt) periodicity with the enhanced peaks corresponding to the start and stop sites, and depict the expected coverage of −12 and −15 nucleotide position for the initiation P-site and termination A-site respectively, as it has been shown for high quality *A. thaliana* RPF libraries (Hsu et al., 2016). We found a very strong periodicity for the fragments of 27 and 28 nucleotides in all the libraries, therefore, we selected those reads for further analysis.

3.3 | The transcriptome and translatome landscapes of germinated pollen at optimum temperature

The gene-specific read counts for RNA and RPF were normalized using the *transcript per kilobase million* (TPM), as it shows better consistency than *reads per million per kilobase* (RPKM) normalization for comparisons among different samples (Li, Ruotti, Stewart, Thomson, &

13653040, 2021, 7, Downloaded from https://onlinelibrary.wiley.com/doi/10.1111/pce.13972 by Bilecik Seyh Edebali, Wiley Online Library on [17/12/2025]. See the Terms and Conditions (https://onlinelibrary.wiley.com/terms-and-conditions) on Wiley Online Library for rules of use; OA articles are governed by the applicable Creative Commons License

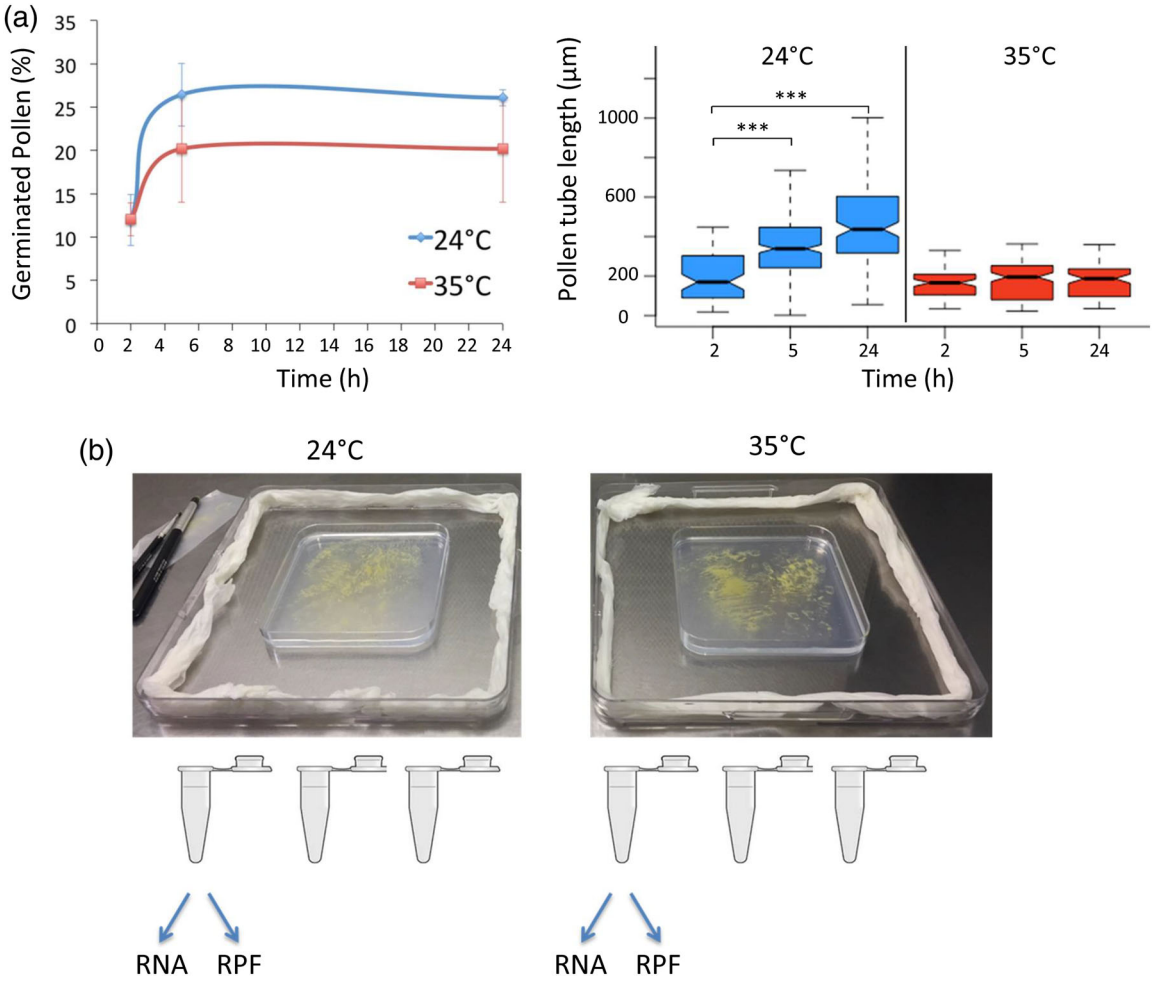

FIGURE 1 Protocol for riboprofiling of germinated pollen at different temperatures. A, time course of germination rate and pollen tube growth were scored for at least 250 and 75 pollen grains respectively. Error bars represent standard deviation of three independent experiments, and asterisks indicate significant differences ($p < .001$) with respect to time 2 h after *t*-test analysis of the same biological replicates. B, rehydrated pollen was germinated and grown in humid chambers at two different temperatures for the simultaneous isolation of total RNA and ribosome-protected RNA fragments (RPF) from three biological replicates

Dewey, 2010; Wagner, Kin, & Lynch, 2012). The complete set of raw counts and normalized TPM data for the *A. thaliana* genome have been deposited at GEO with the accession number GSE145795. Although a minimum value of 1 TPM has been established as a threshold to qualify a gene as expressed in other plant tissues (Hofmann, Schon, & Nodine, 2019) and metazoans (Hebenstreit et al., 2011), we chose the more conservative value of 2 TPM. We then defined the *A. thaliana* pollen transcriptome at 24°C as the set of genes having at least 2 TPM in the average of the 3 replicates of RNA samples at 24°C, with the condition that at least 2 of the 3 replicates should also score a minimum of 2 TPM values. The table of 6,098 genes corresponding to the germinated *A. thaliana* pollen transcriptome at 24°C can be found as Table S1_Tab1.

With the aim to validate our transcriptome list of germinated pollen at 24°C, we first checked the expected absence of photosynthetic genes in our samples of heterotrophic tissue by analysing the expression values of 30 light-harvesting complex genes of photosystem I and II (Umate, 2010) and we found all of them either not detectable or with TPM values close to zero. Next, we compared the transcriptome gene list with previously reported Arabidopsis pollen gene expression at different developmental stages (Borges et al., 2008; Honys & Twell, 2004; Loraine, McCormick, Estrada, Patel, & Qin, 2013; Pina, Pinto, Feijó, & Becker, 2005; Qin et al., 2009; Rutley & Twell, 2015; Wang et al., 2008). To find the common set of pollen transcriptome genes among the different gene lists, we used the UpSetR bioinformatics tool to visualize the intersecting sets (Conway, Lex, & Gehlenborg, 2017). Figure 2A shows the number of genes for all possible intersections among the different lists, with 2,825 genes common to all of them. In addition to the set of genes common to all datasets, our defined pollen transcriptome gene list also includes genes catalogued as pollen-expressed genes in the different published sets. The differences very likely account for variations among the pollen developmental stage, growth conditions, RNA extraction procedures and the technologies used (microarrays versus RNA-Seq), but also for the threshold values used to define a gene as being expressed. To further check whether the set of genes properly

13653040, 2021, 7, Downloaded from https://onlinelibrary.wiley.com/doi/10.1111/pce.13972 by Bilecik Seyh Edebali, Wiley Online Library on [17/12/2025]. See the Terms and Conditions (https://onlinelibrary.wiley.com/terms-and-conditions) on Wiley Online Library for rules of use; OA articles are governed by the applicable Creative Commons License

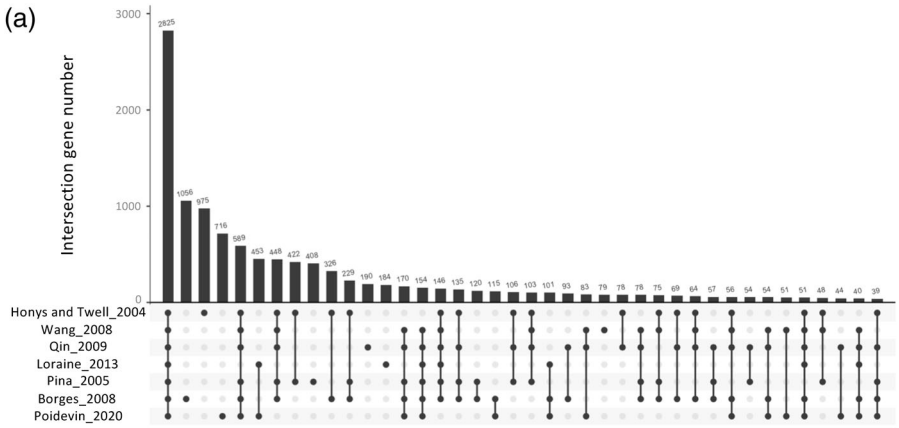

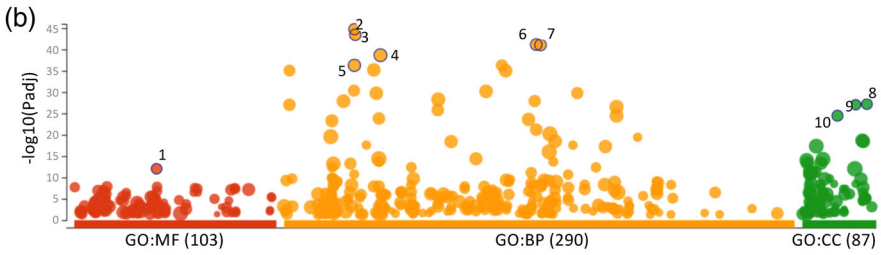

ID	Term ID	Term Name	padj
1	GO:0030599	pectinesterase activity	8.637×10^{-13}
2	GO:0009860	pollen tube growth	1.695×10^{-45}
3	GO:0009932	cell tip growth	3.448×10^{-44}
4	GO:0016192	vesicle-mediated transport	2.110×10^{-39}
5	GO:0009856	pollination	5.140×10^{-37}
6	GO:0048588	developmental cell growth	6.830×10^{-42}
7	GO:0048868	pollen tube development	8.434×10^{-42}
8	GO:0120025	plasma membrane bounded cell projection	6.232×10^{-28}
9	GO:0090406	pollen tube	8.736×10^{-28}
10	GO:0042995	cell projection	3.234×10^{-25}

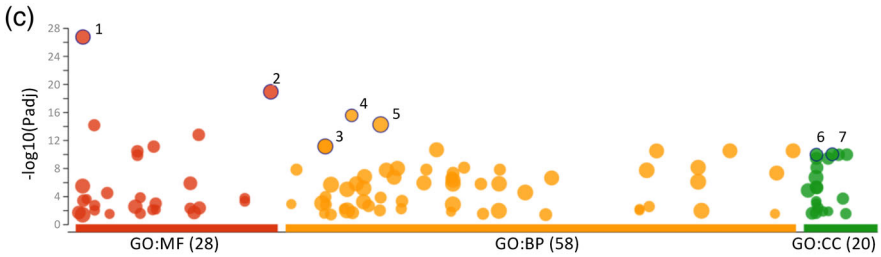

ID	Term ID	Term Name	padj
1	GO:0003700	DNA-binding transcription factor activity	1.914×10^{-27}
2	GO:0140110	transcription regulator activity	1.258×10^{-19}
3	GO:0006351	transcription, DNA-templated	7.765×10^{-12}
4	GO:0009451	RNA modification	2.951×10^{-16}
5	GO:0016070	RNA metabolic process	5.941×10^{-15}
6	GO:0009535	chloroplast thylakoid membrane	1.160×10^{-10}
7	GO:0034357	photosynthetic membrane	1.023×10^{-10}

FIGURE 2 Characterization of the germinated pollen transcriptome at optimum temperature. (A) The UpSetR tool was used to identify the intersection set of genes (black dots) among previously published pollen transcriptomes compared with our own transcriptome gene list. Unique set of genes are indicated by unconnected dots. (B) The Manhattan plot of the enrichment of GO terms in our transcriptome gene list was generated with the g:Profiler toolset highlighting the most significant cases in the different sources indicated by colours. MF refers to "Molecular Function" in red, BP to "Biological Process" in orange, and CC to "Cellular Component" in green. The dot size is proportional to the number of genes included in the term. (C) The g:Profiler plot was used the same way to identify underrepresented GO terms in our transcriptome gene list of germinated pollen at optimum temperature. The GO analysis were performed against the *Arabidopsis thaliana* genome in both cases

define the pollen transcriptome, we used the web-based g:Profiler toolset (Raudvere et al., 2019) to find enriched and underrepresented biological categories in our transcriptome gene list. The results shown in Figure 2B, display the presence of expected overrepresented terms such as "pectinesterase activity," "pollen tube growth," "vesicle-mediated transport" and "cell projection" among others. On the contrary, Figure 2C shows underrepresented GO terms including "transcription regulator activity," "RNA metabolic process," "chloroplast thylakoid membrane" and "photosynthetic membrane," expected down-regulated terms during pollen development.

Once we confirmed that our transcriptome list adequately reflected the mRNA levels of genes involved in pollen germination and growth, we wanted to compare these data with those provided by RPF libraries. These libraries represent the quantitative translational status of the gene set or the translatome, defined as the ribosome-bound mRNA fragments considered to be actively

13653040, 2021, 7, Downloaded from https://onlinelibrary.wiley.com/doi/10.1111/pce.13972 by Bilecik Seyh Edebali, Wiley Online Library on [17/12/2025]. See the Terms and Conditions (https://onlinelibrary.wiley.com/terms-and-conditions) on Wiley Online Library for rules of use; OA articles are governed by the applicable Creative Commons License

translated in a given situation. We defined the *A. thaliana* pollen translatome at 24°C as the set of genes having at least 2 TPM in the average of the 3 replicates of both RNA and RPF samples at 24°C, with the condition that at least 2 of the 3 replicates should also score a minimum of 2 TPM values. The translatome gene list for germinated pollen at 24°C (shown in Table S1_Tab2), accommodates a total of 4,782 genes. We were intrigued by the large list of 1,316 genes absent in the translatome but present in the transcriptome, shown in Table S1_Tab3. Therefore, we performed a GO analysis with this gene list and identified several terms related to "DNA replication," "DNA repair" and "chromosome organization," which are typical GO terms for sperm cells as shown in Figure S3A. In fact, 40% of the 1,316 list of genes are present in the list of sperm genes defined by Borges and coworkers (Borges et al., 2008). Figure S3B shows one example of strong translational repression with the IGV visualization of RNA and RPF reads for the gene AT5G16020 encoding a gamete expressed protein GEX3 only functionally relevant in the female side (Alandete-Saez, Ron, & McCormick, 2008). This indicates that a strict translational regulation occurs during pollen germination to avoid the translation of unnecessary transcripts at this developmental stage.

The use of proteomic approaches has revealed only a modest correlation between mRNA transcript and protein levels (Baerenfaller et al., 2008; Maier, Güell, & Serrano, 2009; Vogel & Marcotte, 2012), therefore, we carried out a correlation plot analysis between the germinated pollen transcriptome and translatome (Figure S4A). The correlation *R* value of 0.88 suggests a rather high correspondence between the transcriptome and the translatome for germinated pollen at 24°C, although some exceptions can be detected. To visualize the differences in the translational profile revealed by the RPF values we used RiboWave (Xu et al., 2018), a pipeline able to denoise the original RPF signal and extract the 3-nt periodicity of the reads known as Periodic Footprint P-site or PF P-site. In Figure S4B we plotted the PF P-site values of two gene examples taken from Figure S4A with similar transcriptional value but obvious differences at the translational level (RPF), the main differences are visualized by alterations in PF P-site values throughout the coding region. The higher translated gene AT5G50030 displays an average of 1,332 PF P-site reads compared to the 124 average reads of AT3G42640. Altogether we have obtained representative gene lists of transcriptome and translatome of *A. thaliana* pollen (Table S1) germinated at optimum temperature (24°C).

3.4 | Transcriptional and translational alterations of germinated pollen by high temperature

The RNA and RPF libraries of germinated pollen at 35°C were computed the same way as it was done previously with the 24°C libraries, allowing us to generate both the transcriptome and translatome gene lists of germinated pollen at 35°C shown in Table S2_Tab1 and Tab2, respectively. Similar to the libraries at optimum temperature, the gene numbers at the restrictive temperature of 35°C were 6,089 for the transcriptome and 4,742 for the translatome. We compared the intersection sets among the 4 gene lists generated (transcriptome 24, translatome 24, transcriptome 35 and translatome 35) using Venn diagrams (Figure 3A). A total of 4,386 genes were common to all 4 sets of genes; 1,415 genes present in the transcriptomes were absent in the translatome lists and 919 genes were exclusively expressed at either 24°C (464 genes) or 35°C (455 genes).

To perform a thorough statistically-based analysis of differential expression for the transcriptomes and translatomes at 24°C and 35°C,

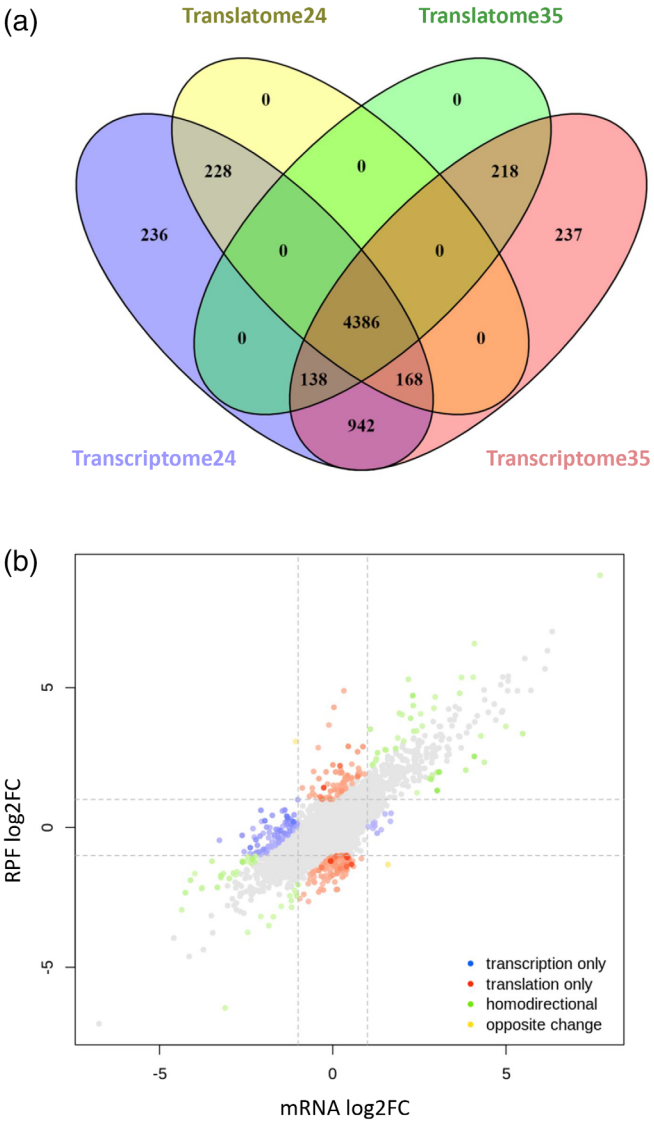

FIGURE 3 Comparative analysis of germinated pollen transcriptomes and translatomes at 24°C and 35°C. (A) Venn diagrams were drawn with the gene lists of transcriptomes and translatomes at both optimum and restrictive temperatures. (B) The graph shows the differential expression analysis correlation obtained with the Xtail pipeline for the transcriptome (RNA log2FC) and the translatome (RPF log2FC) of germinated pollen comparing the treated (35°C) versus the non-treated samples (24°C). The points represent individual genes colour-coded according to their differential values. The intensity of the colour is proportional to the *p*-value, with darker colours indicating more significant *p*-value

13653040, 2021, 7, Downloaded from https://onlinelibrary.wiley.com/doi/10.1111/pce.13972 by Bilecik Seyh Edebali, Wiley Online Library on [17/12/2025]. See the Terms and Conditions (https://onlinelibrary.wiley.com/terms-and-conditions) on Wiley Online Library for rules of use; OA articles are governed by the applicable Creative Commons License

we used the Xtail pipeline, a DESeq2-based protocol with improved sensitivity and accuracy to quantify differential translations with ribosome profiling data (Xiao et al., 2016). To apply the Xtail analysis, we first generated a valid list of genes using only those present in either the translatome 24 or the translatome 35 to avoid invalid data processing for those genes present in transcriptomes but absent in the translatome gene lists. The valid list of genes for Xtail analysis contains 5,138 genes (Table S3). Then we run the Xtail pipeline with

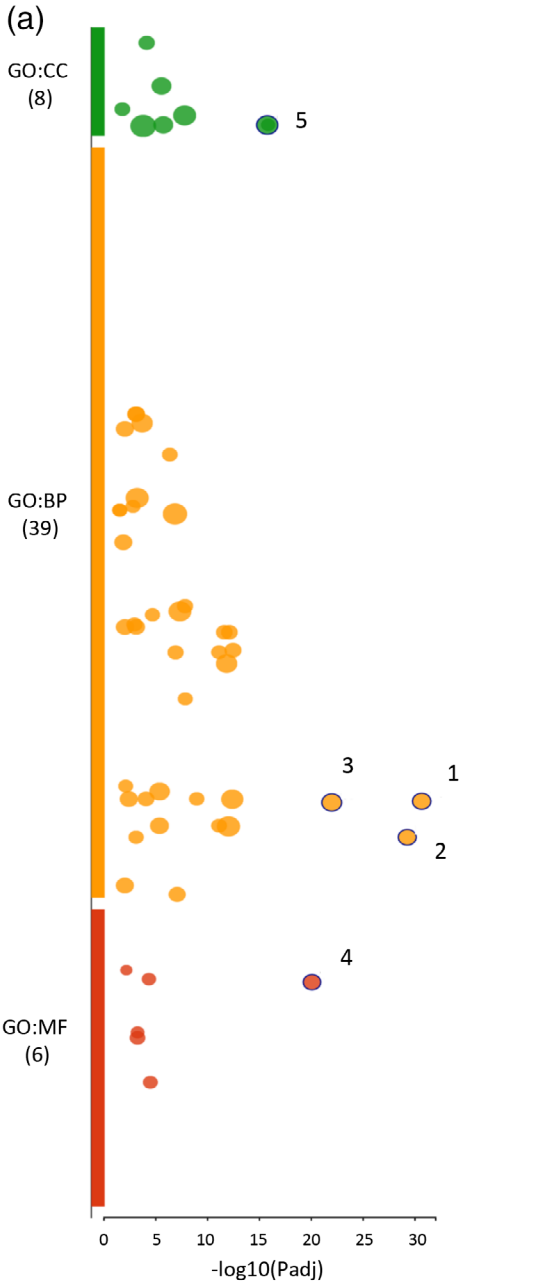

ID	Term ID	Term Name	padj
1	GO:0009408	response to heat	2.599×10^{-31}
2	GO:0006457	protein folding	6.395×10^{-30}
3	GO:0009266	response to temperature stimulus	1.237×10^{-22}
4	GO:0051082	unfolded protein binding	9.971×10^{-21}
5	GO:0005783	endoplasmic reticulum	2.030×10^{-16}

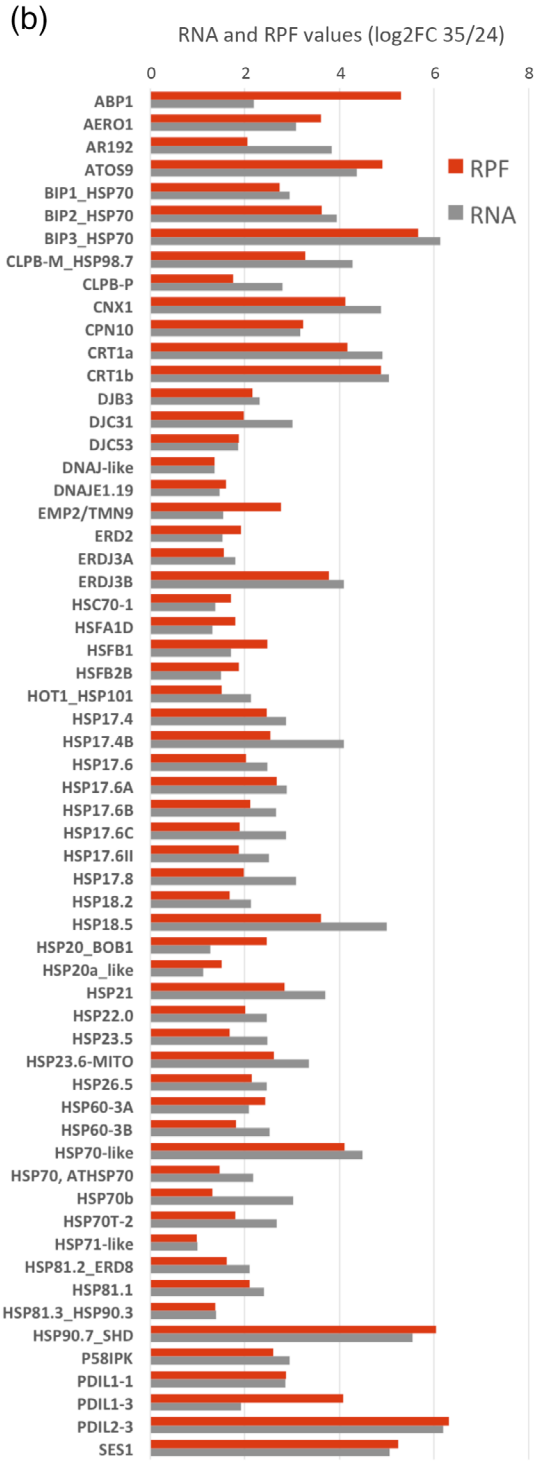

FIGURE 4 GO enrichment of up-regulated genes at high temperature. (A) The g:Profiler tool was used to uncover GO term enrichment of induced genes both at the transcriptional and the translational level, identified through the Xtail analysis. The dot size is proportional to the number of genes included in the term, and the most significant terms are highlighted. The GO enrichment analysis was performed against the custom list of 5,138 valid genes of the Xtail analysis. (B) Shows the graphical representation of log2FC RNA and RPF values for a selected list of genes from the most significant GO terms sorted by gene families

13653040, 2021, 7, Downloaded from https://onlinelibrary.wiley.com/doi/10.1111/pce.13972 by Bilecik Seyh Edebali, Wiley Online Library on [17/12/2025]. See the Terms and Conditions (https://onlinelibrary.wiley.com/terms-and-conditions) on Wiley Online Library for rules of use; OA articles are governed by the applicable Creative Commons License

the valid list of genes to obtain a table (Table S4) that summarizes the quantitative differences at the transcriptional (log2FC mRNA) and translational level (log2FC RPF). Figure 3B displays the plot of transcriptional and translational differences of *A. thaliana* pollen germinated *in vitro* upon heat shock. We found that the vast majority of genes with differential expression (log2FC > 1 or log2FC < −1) display homodirectional changes for the transcriptome and the translatome, with a low number of genes displaying unique transcriptional or translational changes (blue and red coloured dots in Figure 3B). We initially picked those up- or down-regulated genes, both at the translational and transcriptional level, as a proxy for the major increases and reductions of protein levels. According to the restrictive selection criteria, we found 355 up-regulated and 300 down-regulated genes (Table S4). Both lists of genes were analysed with the g:Profiler tool for the presence of enriched terms compared in this case to the valid list of 5,138 genes used for the Xtail analysis.

3.4.1 | Heat up-regulated HSP and ER stress genes.

As it is shown in Figure 4A among the up-regulated genes we could find enriched terms related to "response to heat," "protein folding," "response to temperature stimulus," "unfolded protein binding" and "endoplasmic reticulum." Figure 4B shows the comparison of RNA and RPF log2FC values >1 for a list of representative genes of the most significant GO terms identified, including members of the large heat-shock protein family mostly the small HSP20-like, DNAJ chaperones, ER-related proteins and other members of the unfolded-protein-response (UPR) and the cytosolic-protein-response (CPR) pathways (Table S5).

In a more detailed analysis, Table 1 shows the transcriptional and translational expression levels in germinated pollen for the list of 13 genes co-induced by the three stressor pathways (heat shock, UPR and CPR), previously reported for *A. thaliana* leaves (Sugio et al., 2009). It is remarkable that all the genes are also expressed and induced in germinated pollen upon heat-stress, with the only exception of *AtbZIP60*, a key gene regulator of the UPR pathway (Iwata & Koizumi, 2005) present in germinated pollen although neither transcriptionally nor translationally induced by heat. Altogether the data show that the highly conserved and protective cellular response to heat stress in terms of protein folding seems to be activated in pollen as in vegetative tissues, sharing transcriptional signatures with the related UPR and CPR pathways.

3.4.2 | Heat down-regulated mainly transport genes

On the other hand, we examined the down-regulated list of genes with the aim to identify heat-sensitive pathways. We found strong enrichment of terms defined as "secondary active transmembrane transporter," "active ion transmembrane transporter," or "carbohydrate:proton symporter" all linked to key pathways related to ion homeostasis and secondary transport of carbohydrates coupled to H^+ gradient (Figure 5A). Figure 5B shows the comparison of RNA and RPF log2FC values <1 for transporter genes detailed in Table S6. One paradigmatic case is the enrichment of the cation/H^+ exchangers (CHX) down-regulated upon heat stress. The *CHX* gene family contains 28 members in *A. thaliana* which have been postulated to participate in diverse pollen developmental activities such as ion and metabolite transport, osmotic adjustments, vacuole formation and vesicular trafficking among others (Sze et al., 2004). Although some functional redundancy has been found between CHX transporters (Chanroj, Padmanaban, Czerny, Jauh, & Sze, 2013; Evans, Hall, Pritchard, & Newbury, 2011; Lu et al., 2011), 23 of them displayed >2

TABLE 1 Key genes involved in heat stress and UPR in leaf are UP-regulated in pollen. The table shows normalized values for 13 genes commonly induced by different stressors defined by Sugio, Dreos, Aparicio, and Maule (2009). RNA 24°C, RPF 24°C, log2FC RNA (35°C/24°C) and log2FC RPF (35°C/24°C) are data derived from this work. The last column includes log2FC RNA (37°C/20°C) data obtained from Sugio et al. (2009) [Colour table can be viewed at wileyonlinelibrary.com]

Gene_ID	Gene_description	Gene_symbol	RNA 24C TPM	RPF 24C TPM	RNA Log2FC	RPF Log2FC	Leaf RNA Log2FC
AT1G04980	Protein disulfide isomerase (Leaf)	PDIL2-2	n.d.	n.d.	n.d.	n.d.	1.74
AT1G77510	Protein disulfide isomerase in ER (pollen)	PDIL1-2	1	3	5.19	4.95	n.d.
AT5G64510	Tunicamycin induced 1 protein	TIN1	275	1029	1.21	1.42	5.60
AT4G29330	Der1-like protein involved in degradation in the ER	DER1	2	5	4.54	4.48	3.62
AT4G21810	Der1-like protein involved in degradation in the ER	DER2.1	6	14	2.87	3.33	1.02
AT3G08970	DNAJ domain protein. Thermosensitive male sterile (TMS 1)	ERDJ3A/TMS1	85	217	1.71	1.62	6.01
AT3G62600	DNAJ domain protein in the ER lumen	ERDJ3B	4	7	3.97	3.82	1.03
AT1G56170	DNA-binding Nuclear Factor Y, Subunit C2	NF-YC2	1	1	3.48	4.37	4.87
AT5G03160	DNAJ domain protein in ER lumen	P58IPK	12	32	2.84	2.59	1.02
AT1G42990	ER bZIP DNA binding domain	bZIP60	48	54	0.22	0.67	1.48
AT5G54860	Putative Folate-biopterin transport	MSF-FBT	7	9	1.81	2.23	1.52
AT2G02810	UDP-gal/UDP-glu transporter at the ER	UTR1	7	17	2.19	2.76	1.55
AT1G14360	UDP-gal/UDP-glu transporter on the ER	UTR3	4	5	4.26	4.62	3.40

13653040, 2021, 7, Downloaded from https://onlinelibrary.wiley.com/doi/10.1111/pce.13972 by Bilecik Seyh Edebali, Wiley Online Library on [17/12/2025]. See the Terms and Conditions (https://onlinelibrary.wiley.com/terms-and-conditions) on Wiley Online Library for rules of use; OA articles are governed by the applicable Creative Commons License

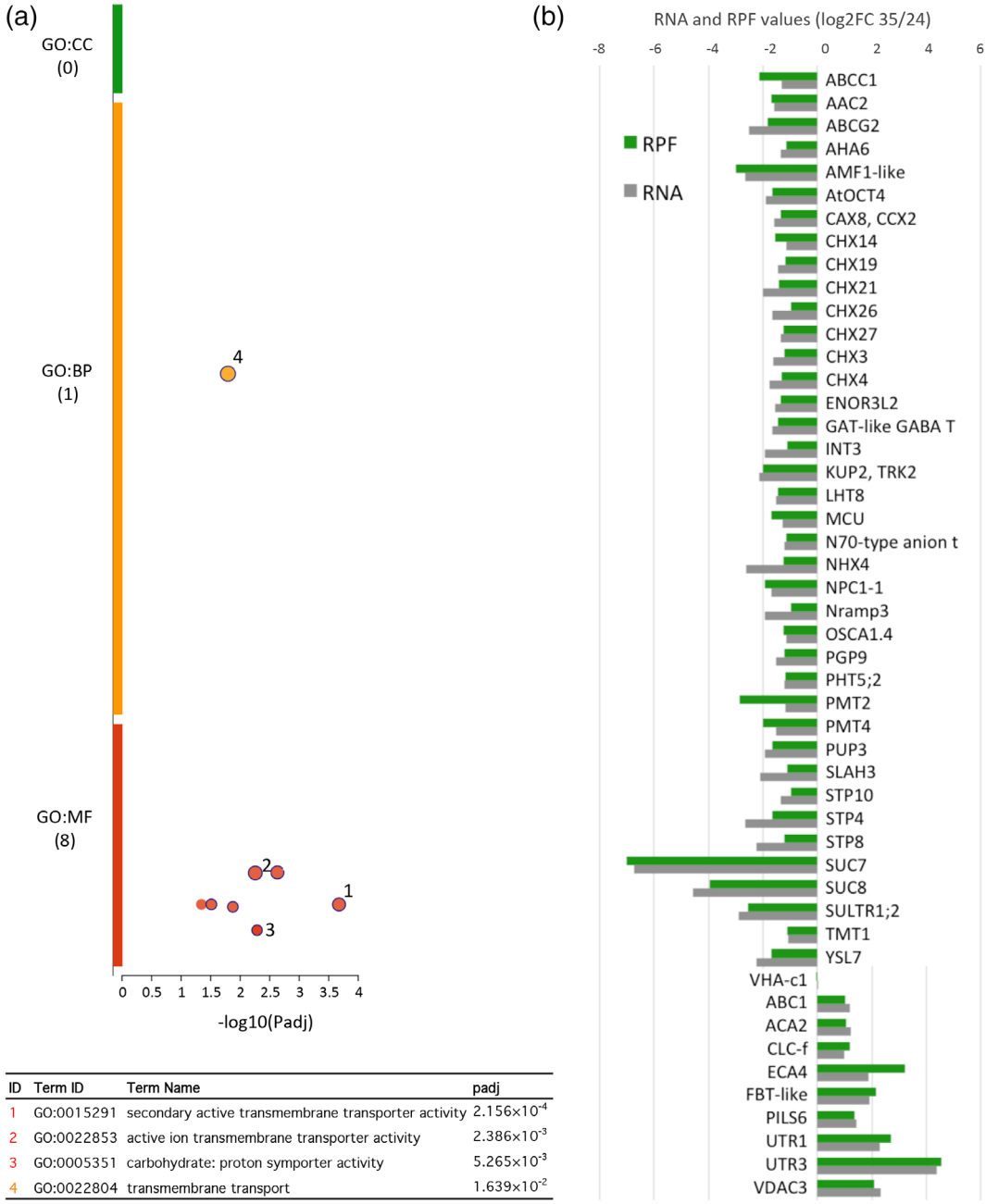

ID	Term ID	Term Name	padj
1	GO:0015291	secondary active transmembrane transporter activity	2.156×10^{-4}
2	GO:0022853	active ion transmembrane transporter activity	2.386×10^{-3}
3	GO:0005351	carbohydrate: proton symporter activity	5.265×10^{-3}
4	GO:0022804	transmembrane transport	1.639×10^{-2}

FIGURE 5 Heat down-regulates mostly membrane transport genes. (A) The g:Profiler tool was used to uncover GO term enrichment of down-regulated genes both at the transcriptional and the translational level, identified through the Xtail analysis. The dot size is proportional to the number of genes included in the term, and the most significant terms are highlighted. The GO enrichment analysis was performed against the custom list of 5,138 valid genes of the Xtail analysis. (B) Shows the graphical representation of log2FC RNA and RPF values for a selected list of genes from the most significant GO terms sorted by gene families

TPM values in both 24°C and 35°C transcriptomes and, therefore, can be considered as *bona fide* members of the germinated pollen transcriptome.

Most of the *CHX* gene family members display a down-regulation both at the transcriptome and translatome levels although only seven members display values below our stringent cutoff (log2FC < 1) as shown in Figure 5B. In addition to the *CHX*s, another gene family negatively affected by elevated temperature at the transcriptional and translational level during pollen germination is the sucrose/H^+ transporter family. Arabidopsis has 9 genes encoding sucrose/H^+ symporters (*AtSUC1-AtSUC9*) mostly expressed in sink tissues and phylogenetically distributed in three subtype groups (Sauer, 2007). Our transcriptome and translatome data indicate that 5 out of the 9 gene family members are transcribed and 4 of them properly translated at optimum temperature, but most of the members display negative log2FC values for transcriptome and translatome. In fact, two of

13653040, 2021, 7, Downloaded from https://onlinelibrary.wiley.com/doi/10.1111/pce.13972 by Bilecik Seyh Edebali, Wiley Online Library on [17/12/2025]. See the Terms and Conditions (https://onlinelibrary.wiley.com/terms-and-conditions) on Wiley Online Library for rules of use; OA articles are governed by the applicable Creative Commons License

them (*AtSUC7* and *AtSUC8*) show the top-ranking values of down-regulated genes by heat stress according to the results of the Xtail analysis (Table S4). In a similar manner, the related family of hexose transporters STP is negatively affected by temperature with three members displaying negative log2FC values <1. In addition to these predominant gene families, the list of membrane transporters down-

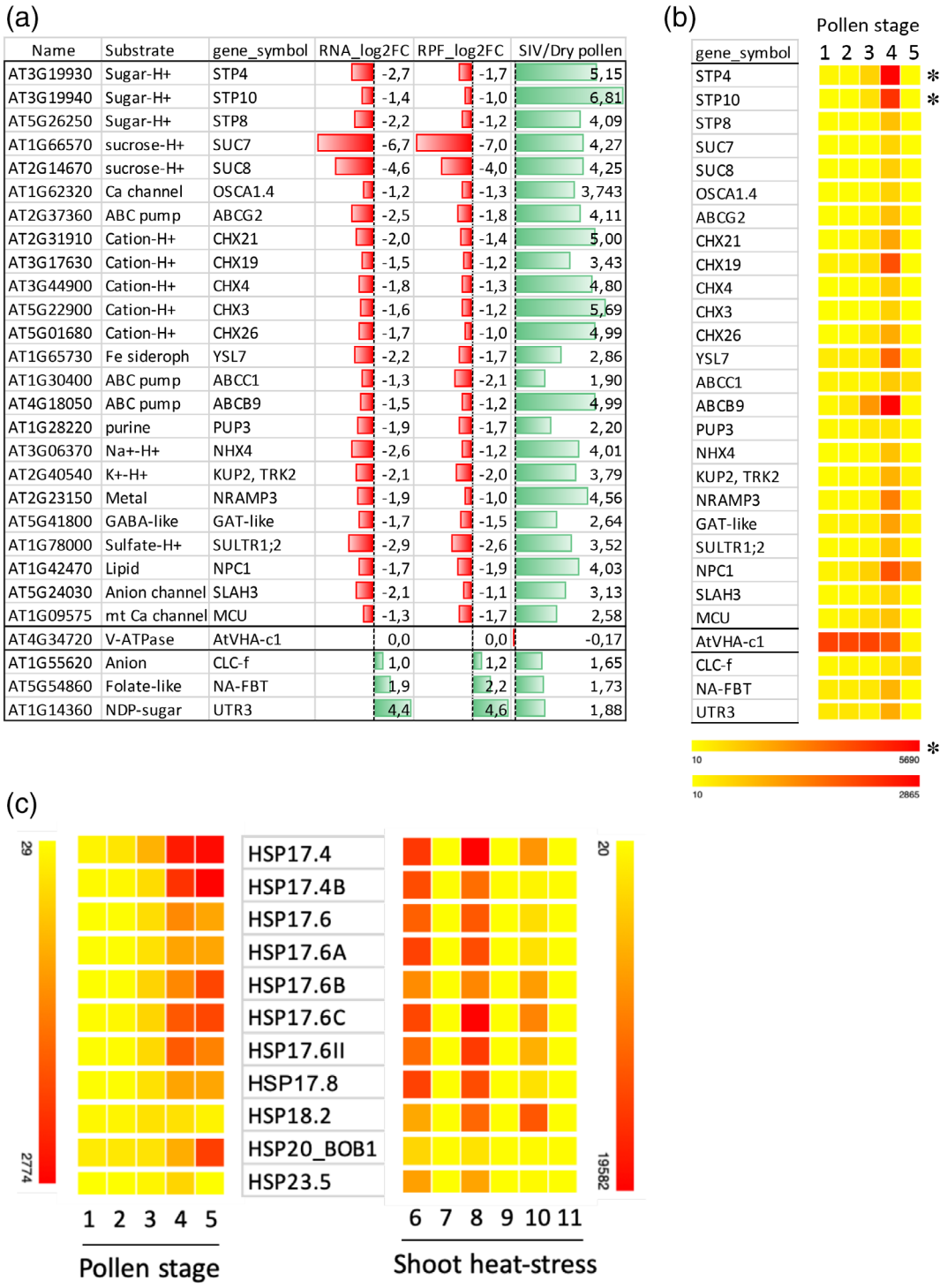

Name	Substrate	gene_symbol	RNA_log2FC	RPF_log2FC	SIV/Dry pollen
AT3G19930	Sugar-H+	STP4	-2,7	-1,7	5,15
AT3G19940	Sugar-H+	STP10	-1,4	-1,0	6,81
AT5G26250	Sugar-H+	STP8	-2,2	-1,2	4,09
AT1G66570	sucrose-H+	SUC7	-6,7	-7,0	4,27
AT2G14670	sucrose-H+	SUC8	-4,6	-4,0	4,25
AT1G62320	Ca channel	OSCA1.4	-1,2	-1,3	3,743
AT2G37360	ABC pump	ABCG2	-2,5	-1,8	4,11
AT2G31910	Cation-H+	CHX21	-2,0	-1,4	5,00
AT3G17630	Cation-H+	CHX19	-1,5	-1,2	3,43
AT3G44900	Cation-H+	CHX4	-1,8	-1,3	4,80
AT5G22900	Cation-H+	CHX3	-1,6	-1,2	5,69
AT5G01680	Cation-H+	CHX26	-1,7	-1,0	4,99
AT1G65730	Fe sideroph	YSL7	-2,2	-1,7	2,86
AT1G30400	ABC pump	ABCC1	-1,3	-2,1	1,90
AT4G18050	ABC pump	ABCB9	-1,5	-1,2	4,99
AT1G28220	purine	PUP3	-1,9	-1,7	2,20
AT3G06370	Na+-H+	NHX4	-2,6	-1,2	4,01
AT2G40540	K+-H+	KUP2, TRK2	-2,1	-2,0	3,79
AT2G23150	Metal	NRAMP3	-1,9	-1,0	4,56
AT5G41800	GABA-like	GAT-like	-1,7	-1,5	2,64
AT1G78000	Sulfate-H+	SULTR1;2	-2,9	-2,6	3,52
AT1G42470	Lipid	NPC1	-1,7	-1,9	4,03
AT5G24030	Anion channel	SLAH3	-2,1	-1,1	3,13
AT1G09575	mt Ca channel	MCU	-1,3	-1,7	2,58
AT4G34720	V-ATPase	AtVHA-c1	0,0	0,0	-0,17
AT1G55620	Anion	CLC-f	1,0	1,2	1,65
AT5G54860	Folate-like	NA-FBT	1,9	2,2	1,73
AT1G14360	NDP-sugar	UTR3	4,4	4,6	1,88

FIGURE 6 Down-regulated transporter genes display opposite trend during *SIV* growth. (A) The list of down-regulated membrane transporter genes was scored for their gene expression value ratios of SIV/dry pollen showing reverse tendency to heat-response. (B) The list of down-regulated membrane transporter genes was analysed with the "Arabidopsis Heat Tree Viewer" web tool to represent gene expression according to values indicated in the scales, either with or without asterisk. (C) Small HSPs expressed in pollen were analysed similarly with the "Arabidopsis Heat Tree Viewer" web tool and the scales showed below. Numbers indicate different pollen developmental stages: 1—dry pollen; 2—0.5 h *in vitro* pollen tubes; 3—4 h *in vitro* pollen tubes; 4—*SIV* pollen tubes; 5—sperm; 6—heat 1 h shoot; 7—heat_control 1 h shoot; 8—heat 3 h shoot; 9—heat_control 3 h shoot; 10—heat 4 h shoot; 11—heat_control 4 h shoot

13653040, 2021, 7, Downloaded from https://onlinelibrary.wiley.com/doi/10.1111/pce.13972 by Bilecik Seyh Edebali, Wiley Online Library on [17/12/2025]. See the Terms and Conditions (https://onlinelibrary.wiley.com/terms-and-conditions) on Wiley Online Library for rules of use; OA articles are governed by the applicable Creative Commons License

regulated at high temperature is remarkable including primary membrane-energizing transporters such as AHA 6 which may be highly deleterious for pollen tube growth considering the importance of H^+ homeostasis. In contrast, the vacuolar H^+ ATPase VHA, and many diverse membrane transporters showed little to no significant changes or even induction after the heat shock (Figure 5B). Overall, these data suggest that a failure in the orchestrated presence of at least 39 membrane transporters under heat stress could be detrimental for proper germination and growth of the pollen tube.

To gain further insight into the roles of the heat-sensitive membrane transporters, we checked their expression during pollen development, as previous studies showed specific expression patterns during pollen maturation (Bock et al., 2006). We used transcriptome data published by others (Borges et al., 2008; Qin et al., 2009) showing expression of *A. thaliana* pollen in different stages: dry pollen, pollen germinated *in vitro* at two different times (0.5 and 4 h), pollen germinated *semi in vivo* (*SIV*) and sperm cells. Germinated pollen includes a vegetative tube cell and two sperm cells, and when germinated in *SIV* condition refers to pollen tubes emerged from a cut style on nutrient medium after germinated on a stigma (Qin et al., 2009). As shown in Figure 6A, we found a striking relationship between a subset of heat-down regulated transporters in our analysis and their up-regulation in *SIV* germinated tubes at basal temperature compared to dry pollen.

To further illustrate this finding, we used the web-based tool "Arabidopsis Heat Tree Viewer" to compare five different pollen developmental stages. As it can be seen in Figure 6B, there is a notable up-regulation of gene expression for at least 23 transporters after 4 h *in vitro* growth and especially in tubes grown under *SIV*. We also checked the expression during these five pollen stages of the heat-induced genes identified previously in our dataset, to find co-regulated patterns, and we focused on the 17 pollen-expressed genes induced by heat belonging to the conserved family of the small heat shock proteins (sHSPs) in plants (Scharf, Siddique, & Vierling, 2001; Waters, 2012). We found that 11 of them displayed a similar pollen gene expression pattern to the transporters, with increased expression during *in vitro* germination further enhanced in *SIV* conditions, whereas in shoots, although highly induced by heat, their basal expression is null (Figure 6C). These data suggest that during pollen germination there is a strong requirement for expression of key ion and carbohydrate transporters together with proteins involved in folding and refolding, and, during heat stress conditions, in spite of a proper induction of the folding machinery, a lack of gene expression response for the transporters may lead to pollen tube growth defects.

To further verify the gene expression data obtained by deep sequencing, we selected 4 up- and 4 down-regulated genes to validate the data with RTqPCR analysis. After rehydration, pollen was grown for 5 h both at 24°C and 35°C. In addition, to differentiate the effect of heat on germinated pollen, we run in parallel another in vitro test where pollen was grown for 3 h at 24°C and then shifted to further 2 h at 35°C (sample 24_35). The data obtained are shown in Figure 7. We could reproduce the sequencing data with the RTqPCR

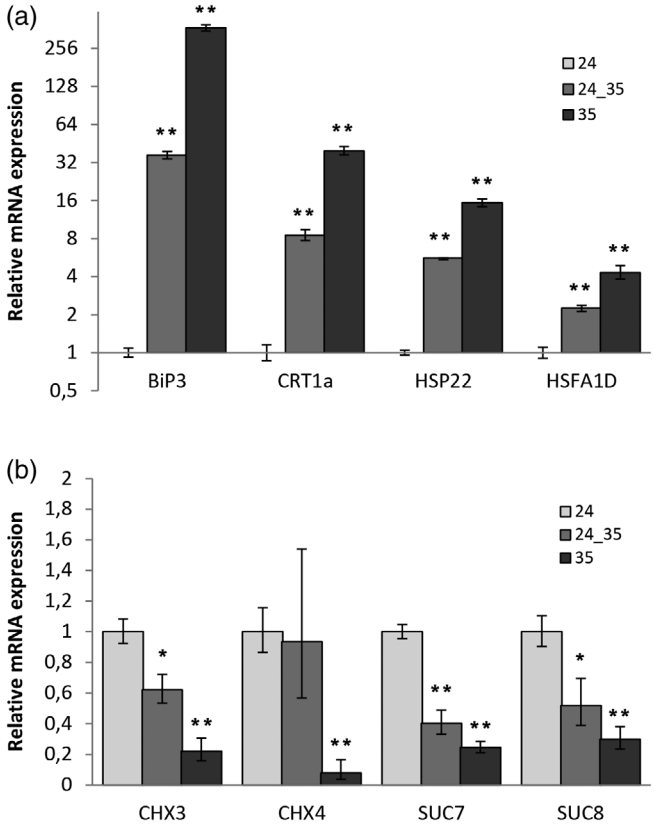

FIGURE 7 Validation of gene expression by RTqPCR. Total RNAs were isolated from pollen grown in vitro for 5 h at 24°C (24), 5 h at 35°C (35) and 3 h at 24°C and then shifted to 35°C for two additional hours (24_35). RTqPCRs were performed for heat up-regulated genes (A) and heat down-regulated genes (B) as indicated. The values were normalized to the YSL8 gene and to the 24 control sample. Expression levels are represented as the mean ± SD of two biological replicates. Statistical analysis with *t*-test are shown with one asterisk (*) or two asterisks (**) for the significant differences with the control sample (24) with $p < .05$ and $p < .001$ respectively

analysis when comparing the 24 and 35 samples for the up- and down-regulated genes. In the case of the shifted sample (24_35) the data also confirm the results for the up-regulated genes indicating that germinated pollen at optimum temperature does respond to the heat treatment. The data obtained for the down-regulated genes also confirm the down-regulation by heat although the differences are not so dramatic. A plausible explanation for these cases is that the mRNA half-life also accounts for the amount of mRNA present in the sample in particular for short heat treatments.

3.4.3 | Changes in translational efficiency during heat stress

We analysed whether Riboprofiling revealed any alteration in translational efficiency (TE), referred to the changes in the ratio of RPF to RNA counts for a given gene between two different conditions. The

13653040, 2021, 7, Downloaded from https://onlinelibrary.wiley.com/doi/10.1111/pce.13972 by Bilecik Seyh Edebali, Wiley Online Library on [17/12/2025]. See the Terms and Conditions (https://onlinelibrary.wiley.com/terms-and-conditions) on Wiley Online Library for rules of use; OA articles are governed by the applicable Creative Commons License

TABLE 2 Different scenarios account for TE changes. Symbols (–), (+) and (=) indicate a reduction, increase or no change in gene expression, respectively. The numbers are relative to the total number of differentially expressed genes (5138)

log2FC RNA	log2FC RPF	TE Up (# genes)	TE Up (%)	TE Down (# genes)	TE Down (%)
–	–	16	13.3	2	2.6
+	–	0	0	1	1.3
=	–	0	0	45	58.4
–	+	2	1.7	0	0
+	+	9	7.5	9	11.7
=	+	28	23.3	0	0
–	=	52	43.3	0	0
+	=	0	0	1	1.3
=	=	13	10.8	19	24.7
Sum (% pollen translatome)		120	2.3	77	1.5

Xtail algorithm uses two parallel pipelines to quantify the TE changes, first as the difference between the log2FC of RPF and RNA across the two temperature conditions, and second as the difference between the log2 ratios of RPF to RNA in both conditions (log2Rs). Both calculations should yield a similar result, and the more conserved pipeline with better p-value is selected for the final assessment (log2FC_TE) of differential translation (Xiao et al., 2016). Figure S5A shows the correlation plot of log2Rs at 24°C and 35°C where a notable homodirectional pattern, similar to the transcriptome versus translatome shown in Figure 3B, can be observed. In spite of some exceptions (coloured dots in Figure S5A), most of the alterations in TE occur for RNA and RPF in a correlated manner, therefore we see no evidence of wide effects of high temperature on translation dynamics. According to acceptable p-value < .05 we found 77 and 120 genes with down-regulated or up-regulated log2FC_TE values, respectively (Table S4). In spite of the low number of genes affected (3.8%), we investigated the nature of those changes by considering all possible regulatory scenarios. Table 2 shows a summary of all the 9 possible changes at either the RNA or RPF between both temperatures that may lead to final TE changes.

As it can be seen, among the down-regulated TE genes, a large number (58.4%) show changes caused by RPF with no RNA alterations, suggesting specific translational inhibition mechanisms. Intriguingly, the case is the opposite for a large proportion (43.3%) of the up-regulated TE genes with most of the changes affecting at the RNA level. The graphical representation of log2FC_TE as a function of the p-value is shown in the volcano plot of Figure S5B. Some exceptions to the homodirectional pattern are the ATP-dependent caseinolytic (Clp) protease (AT1G09130) which suffers a strong down-regulation at the translational level with the increase in temperature, or the annotated as non-coding RNAs AT5G06845 and AT1G05853 with surprisingly enhanced ribosome footprints at 35°C. In fact, the top three genes with up regulated log2FC_TE values are non-coding RNAs with RPF values unexpectedly increased at 35°C (Table S4). The functional interpretation of RPF reads on annotated non-coding RNAs remains to be clarified and is considered in the next section.

3.5 | Revisiting predicted functions and annotations for the translatome of germinated pollen

In spite of experimental and bioinformatics removal of rRNAs, tRNAs, snRNAs and snoRNAs, our transcriptome and translatome lists contained genes annotated as non-coding RNAs. These include mostly long-non-coding RNAs, transposable elements and a few small-nucleolar RNAs that probably escaped the filtering due to annotation issues. Apart from their possible roles as regulatory transcripts with transcriptional and post-transcriptional impact, some of these RNAs show significant RPF reads suggesting the presence of ribosomes according to the very strict RPF size used in the analysis (only 27 and 28 nt long). One paradigmatic example is the gene AT2G41310 with very high transcriptome values both at 24°C and 35°C, but very low RPF values (Tables S3 and S4). This gene, annotated as ARR8/ATRR3, encodes an A-type response regulator involved in cytokinin-mediated signalling, and it caught our interest as it was not expected to be expressed in pollen. Figure S6A shows the IGV coverage data showing that the reads fall into the 3′ untranslated region overlapping with a non-coding RNA (AT2G09250) in the opposite orientation. Therefore, there is no doubt that read coverage in that region does not correspond to the encoded ARR8 protein. We then used the Ribowave pipeline to examine the periodicity of PF P-sites in that region. The results shown in Figure S6B demonstrate the presence of periodic P-site footprints at both temperatures matching different putative open reading frames, thus suggesting that this gene could be translated in germinated pollen. Similar observations were found for other non-coding-RNAs showing detectable RPF reads in the genes AT5G06845 and AT1G05853, however, the limiting PF P-site density and low coverage values in most of these cases precludes the achievement of any definitive conclusion as to whether those genes are indeed translated.

4 | DISCUSSION

In this work we have used a high-resolution ribosome profiling technology to achieve a comprehensive study of how heat affects both

13653040, 2021, 7, Downloaded from https://onlinelibrary.wiley.com/doi/10.1111/pce.13972 by Bilecik Seyh Edebali, Wiley Online Library on [17/12/2025]. See the Terms and Conditions (https://onlinelibrary.wiley.com/terms-and-conditions) on Wiley Online Library for rules of use; OA articles are governed by the applicable Creative Commons License

the transcriptome and the translatome of *A. thaliana in vitro* germinated pollen. In the course of this work, we found some limitations of using *in vitro* germinated pollen after cold-storage, needed to accomplish the large-scale pollen collection required for the Riboprofiling analysis. For instance, a large number of pollen grains do not complete germination even under optimum growth conditions after cold-storage, but still the percentage of germinated pollen grains (with highly reproducible tube growth behaviour) is sufficient to evaluate gene expression according to the data obtained. Another example illustrating the validity of our approach is that the transcriptome and translatome changes shown are largely affecting the pollen vegetative cell, and in fact, we have observed strong translational repression of GO terms specific for sperm cells that under those conditions would be inactive as the case example gene *GEX3* (Figure 3B). The gene *GEX3*, known to be transcriptionally active in both male and female gametophytes, showed no phenotypic alteration for pollen development when down-regulated, and the analysis of gamete-specific *GEX3* antisense and overexpression transgenic lines had reduced seed set caused exclusively by defects on the female gametophyte (Alandete-Saez et al., 2008). Other strategies to characterize the Arabidopsis pollen translatome *in vivo* followed different experimental approaches, like the use of transgenic plants expressing tagged ribosomal genes from heterologous pollen promoters and the isolation of mRNAs co-precipitating with ribosomal subunits; leading to a rather different dataset (Lin et al., 2014) as one would expected for too many differences in the nature of the biological samples, the processing and the downstream technologies implemented.

Our results provide novel insights on the effects of high temperature on pollen gene expression after obtaining a complete dataset of the transcriptome and the translatome of *in vitro* germinated pollen at basal (24°C) and restrictive temperature (35°C). The differential expression analysis uncovered new findings that can be summarized as follows: (i) the conserved cellular machinery to cope with heat stress is well functioning in germinated pollen, as we found up-regulated many genes of the heat-response, the UPR and the CPR pathways; (ii) the enrichment of membrane transporters, involved in ion and carbohydrate transport among the down-regulated genes, identified heat-sensitive targets; (iii) we detected a co-regulation between heat-sensitive membrane transporters and heat-induced proteins during specific stages of pollen germination, namely *in vitro* and *SIV*, illustrating new co-regulatory aspects of pollen germination; (iv) although we found a high correlation between transcription and translation, specific translational efficiency alterations could also be uncovered in germinated pollen; and (v) we could detect the presence of ribosome footprints on non-coding RNAs, illustrating the need of further refinement for gene expression on germinated pollen.

An important question concerns the nature of the up- and down-regulation gene expression patterns. As we have monitored RNA and RPF levels in response to heat, it is unclear whether their alterations are due to changes in the synthesis or degradation, or both. Pollen grains contain stored mRNA, and it is assumed the mRNAs can be released and immediately translated after pollination to support rapid tube growth (Mascarenhas, 1993). Recent data have shown the presence of cytoplasmic mRNA granules, namely stress granules (SGs), in mature pollen grains co-localizing with processing body (PB) proteins, thus suggesting the presence of PBs during pollen maturation (Scarpin et al., 2017). Both SGs and PBs are intimately connected with each other and with the translational machinery, to modulate the mRNA turnover during stress conditions (Chantarachot & Bailey-Serres, 2018). Thus, an increase in transcript could reflect a combination of newly synthesized transcripts and released mRNAs from storage granules, and a down-regulation could be caused by reduced transcription or enhanced degradation in PBs, or both. The experiments shown in Figure 7 with germinated pollen at 24°C for 3 h and shifted for additional 2 h at 35°C suggest that mRNA turnover may impact at higher extent for down-regulation of gene expression, although this will require future experiments to quantify mRNA half-lives.

The differential gene expression analysis provided clues on the cellular pathways up-regulated and down-regulated by heat stress. Among the up-regulated pathways, we could find a significant enrichment of GO terms related to heat shock response, protein folding and quality control ER-dependent pathways demonstrating that *A. thaliana* pollen tube is able to sense and respond to heat stress in a similar manner to ER-dependent stress responses in leaves (Sugio et al., 2009). As a step to identify the molecular basis of heat sensitivity, we studied enriched GO terms of down-regulated genes. We focused on membrane transporters, as they were enriched among the 300 genes down-regulated by heat. Over 260 transporter genes expressed in germinated pollen we found 39 of them (14.8%) down-regulated, so for the majority of transporters, including the vacuolar H^+ pump ATPase VHA, heat had little effect. However, down-regulation of those 39 genes affected to transporters with key functions during pollen tube growth, including the primary pump H^+-ATPase AHA6, calcium channels like OsCA1.4, ABC pumps and H^+-coupled secondary transporters for K^+, anions (sulfate, phosphate), metals and amino acid transporters like LHT8. Most prominent is the large number of H^+-coupled sugar transporters (*SUC* and *STP* genes) and members of the cation/H^+ exchanger family (*CHXs*) with most of their family members affected. Altogether, the massive down-regulation of membrane transporters by heat may lead to devastating consequences due to the strong requirements of highly active vesicular transport during pollen tube growth.

We also discovered that about two thirds of these down-regulated transporters by high temperature are also up-regulated during *in vitro* germination and especially when pollen tubes were grown under *semi in vivo* (*SIV*) conditions (Qin et al., 2009). Increased expression of sucrose and hexose transporters likely provides carbon source for energy and for synthesizing pollen walls, but also signalling roles have been proposed (Rottmann, Fritz, Sauer, & Stadler, 2018a). So, is there any relationship between down-regulation of transporters by heat and their up-regulation by germination conditions? We have shown that, as in leaves, germinated pollen stressed by heat also triggers up-regulation of folding (chaperone HSPs) and quality control pathways, and many of those up-regulated genes are also induced under *in vitro* and in *SIV* germination conditions. One prevalent

13653040, 2021, 7, Downloaded from https://onlinelibrary.wiley.com/doi/10.1111/pce.13972 by Bilecik Seyh Edebali, Wiley Online Library on [17/12/2025]. See the Terms and Conditions (https://onlinelibrary.wiley.com/terms-and-conditions) on Wiley Online Library for rules of use; OA articles are governed by the applicable Creative Commons License

example is the family of cytoplasmic small HSPs (sHSPs), abundantly expressed in germinated pollen under heat stress as they are required to prevent protein aggregation. We have found that 13 out of 17 pollen expressed sHSPs are also induced during *SIV*, thus uncovering potential roles of these chaperones in the germination process. One of these chaperones, the sHSP BOB1 protein, was found incorporated into heat shock granules (HSGs) at high temperature (Perez et al., 2009). Therefore, we cannot discard that assembly of HSGs, stress granules and processing bodies may lead to either sequestration or targeted degradation of specific mRNAs instead of inhibition of transcription, to explain the gene down-regulation of transporters upon heat stress in germinated pollen.

An advantage of the Riboprofiling technology is that simultaneous identification of mRNA and RPFs allows the quantification of changes in translational efficiency (TE). The differential analysis of TE upon heat stress revealed that only a minor subset of genes displayed significant TE alterations. The sources of TE alterations are very diverse since they may affect to either RNA or RPF levels both at 24°C and 35°C. It is remarkable that, among the TE down-regulated genes, most of them include changes exclusively in the RPF, as an indication of translation-specific repression. On the other side, among the TE up-regulated genes, almost half of them are caused by changes in RNA levels. The nature of the translational regulations remains to be elucidated.

In addition to detecting gene expression changes, Riboprofiling analysis allows the direct observation of the precise mapping positions of the reads, using integrated visualization programs such as IGV. For instance, a questionable annotation could lead to erroneous hypothesis in the case of the ARR8 encoded gene (AT2G41310). Another example is the case of *AtSUC7*, initially considered as a pseudogene (Sauer et al., 2004), and recently shown to be translated in heterologous systems with functional restrictions on sucrose analogue transport (Rottmann et al., 2018b). Here we show that *AtSUC7* is transcribed and translated in germinated pollen and it suffers a dramatic down regulation at both transcriptional and translational levels upon heat stress. The Riboprofiling of *A. thaliana* germinated pollen has also uncovered the unexpected presence of RPF reads on several non-coding-RNAs, such as long-non-coding-RNAs and small-nucleolar-RNAs. Additional experimental and functional data will be required to unequivocally show that those non-coding-RNAs are indeed subjected to translation during pollen germination and growth.

As a conclusion, we can affirm that the use of *in vitro* germinated pollen is a useful system to understand the molecular basis of heat-induced responses. Riboprofiling has provided many answers to better understand pollen gene expression responses, as for instance the particular sensitivity of transporters to the heat insult. Our gene expression data, combined with previously reported information on *SIV* germinated pollen, suggests that pollen tube growth is fully armed, with the co-induction of heat-chaperone proteins and transporters, to cope with a high demand of vesicle transport and resilience to environmental and/or female cues during its journey to the ovule. However, it has also raised many questions that remain to be addressed like the nature of the regulatory molecular mechanisms involved and the translation of annotated genes as non-coding RNAs. The implementation of this powerful technology to the diverse pollen developmental stages and environmental cues in future studies, will provide a more detailed picture of this key aspect of plant biology as it is the fertilization process in a constantly changing environment.

ACKNOWLEDGMENTS

The authors thank the Bioinformatics Core Service of the IBMCP for technical assistance. We also thank José M. Alonso, Anna Stepanova, René Toribio and Mar Castellano for sharing protocols with helpful advices on ribosome profiling, and for critical reading of the manuscript. We also thank Gad Miller and Nick Rutley for sharing data and stimulating discussions. We are indebted to Heven Sze (University of Maryland) for giving extraordinary input with transporter gene nomenclature and expression and very useful ideas to improve the quality of the manuscript. We also thank Mark A. Johnson (Brown University) for the development of the tool "Arabidopsis Heat Tree Viewer."

CONFLICT OF INTEREST

The authors declare that the research was conducted in the absence of any commercial or financial relationships that could be considered as a potential conflict of interest.

ORCID

Alejandro Ferrando https://orcid.org/0000-0002-1903-9111

REFERENCES

Ahmed, M., & Kim, D. R. (2018). PCR: An R package for quality assessment, analysis and testing of qPCR data. *PeerJ*, *6*, e4473. https://doi.org/10.7717/peerj.4473

Alandete-Saez, M., Ron, M., & McCormick, S. (2008). GEX3, expressed in the male gametophyte and in the egg cell of *Arabidopsis thaliana* is essential for micropylar pollen tube guidance and plays a role during early embryogenesis. *Molecular Plant*, *1*(4), 586–598.

Anders, S., Pyl, P. T., & Huber, W. (2014). HTSeq—A Python framework to work with high-throughput sequencing data. *Bioinformatics*, *31*(2), 166–169. https://doi.org/10.1093/bioinformatics/btu638

Baerenfaller, K., Grossmann, J., Grobei, M. A., Hull, R., Hirsch-Hoffmann, M., Yalovsky, S., … Baginsky, S. (2008). Genome-scale proteomics reveals *Arabidopsis thaliana* gene models and proteome dynamics. *Science*, *320*(5878), 938–941.

Begcy, K., Nosenko, T., Zhou, L.-Z., Fragner, L., Weckwerth, W., & Dresselhaus, T. (2019). Male sterility in maize after transient heat stress during the tetrad stage of pollen development. *Plant Physiology*, *181*(2), 683–700. https://doi.org/10.1104/pp.19.00707.

Boavida, L. C., & McCormick, S. (2007). Technical advance: Temperature as a determinant factor for increased and reproducible in vitro pollen germination in *Arabidopsis thaliana*. *The Plant Journal*, *52*(3), 570–582. https://doi.org/10.1111/j.1365-313X.2007.03248.x

Bock, K. W., Honys, D., Ward, J. M., Padmanaban, S., Nawrocki, E. P., Hirschi, K. D., … Sze, H. (2006). Integrating membrane transport with male gametophyte development and function through transcriptomics. *Plant Physiology*, *140*(4), 1151–1168. https://doi.org/10.1104/pp.105.074708

Borges, F., Gomes, G., Gardner, R., Moreno, N., McCormick, S., Feijó, J. A., & Becker, J. D. (2008). Comparative transcriptomics of

13653040, 2021, 7, Downloaded from https://onlinelibrary.wiley.com/doi/10.1111/pce.13972 by Bilecik Seyh Edebali, Wiley Online Library on [17/12/2025]. See the Terms and Conditions (https://onlinelibrary.wiley.com/terms-and-conditions) on Wiley Online Library for rules of use; OA articles are governed by the applicable Creative Commons License

Arabidopsis sperm cells. *Plant Physiology*, *148*(2), 1168–1181. https://doi.org/10.1104/pp.108.125229

Bou Daher, F., Chebli, Y., & Geitmann, A. (2009). Optimization of conditions for germination of cold-stored *Arabidopsis thaliana* pollen. *Plant Cell Reports*, *28*(3), 347–357. https://doi.org/10.1007/s00299-008-0647-1

Conway, J. R., Lex, A., & Gehlenborg, N. (2017). UpSetR: An R package for the visualization of intersecting sets and their properties. *Bioinformatics*, *33*(18), 2938–2940. https://doi.org/10.1093/bioinformatics/btx364

Cunningham, F., Achuthan, P., Akanni, W., Allen, J., Amode, M. R., Armean, I. M., … Flicek, P. (2018). Ensembl 2019. *Nucleic Acids Research*, *47*(D1), D745–D751. https://doi.org/10.1093/nar/gky1113

Czechowski, T., Stitt, M., Altmann, T., Udvardi, M. K., & Scheible, W. R. (2005). Genome-wide identification and testing of superior reference genes for transcript normalization in Arabidopsis. *Plant Physiology*, *139*(1), 5–17.

Chanroj, S., Padmanaban, S., Czerny, D. D., Jauh, G.-Y., & Sze, H. (2013). K + transporter AtCHX17 with its hydrophilic C tail localizes to membranes of the secretory/endocytic system: Role in reproduction and seed set. *Molecular Plant*, *6*(4), 1226–1246. https://doi.org/10.1093/mp/sst032

Chantarachot, T., & Bailey-Serres, J. (2018). Polysomes, stress granules, and processing bodies: A dynamic triumvirate controlling cytoplasmic mRNA fate and function. *Plant Physiology*, *176*(1), 254–269. https://doi.org/10.1104/pp.17.01468

Chaturvedi, P., Ischebeck, T., Egelhofer, V., Lichtscheidl, I., & Weckwerth, W. (2013). Cell-specific analysis of the tomato pollen proteome from pollen mother cell to mature pollen provides evidence for developmental priming. *Journal of Proteome Research*, *12*(11), 4892–4903. https://doi.org/10.1021/pr400197p

Chebli, Y., Kroeger, J., & Geitmann, A. (2013). Transport logistics in pollen tubes. *Molecular Plant*, *6*(4), 1037–1052.

Chen, Y., & Brandizzi, F. (2012). AtIRE1A/AtIRE1B and AGB1 independently control two essential unfolded protein response pathways in Arabidopsis. *The Plant Journal*, *69*(2), 266–277. https://doi.org/10.1111/j.1365-313X.2011.04788.x

Cheng, C.-Y., Krishnakumar, V., Chan, A. P., Thibaud-Nissen, F., Schobel, S., & Town, C. D. (2017). Araport11: A complete reannotation of the *Arabidopsis thaliana* reference genome. *The Plant Journal*, *89*(4), 789–804. https://doi.org/10.1111/tpj.13415

Cheung, A. Y., & Wu, H.-M. (2007). Structural and functional compartmentalization in pollen tubes. *Journal of Experimental Botany*, *58*(1), 75–82. https://doi.org/10.1093/jxb/erl122

Evans, A. R., Hall, D., Pritchard, J., & Newbury, H. J. (2011). The roles of the cation transporters CHX21 and CHX23 in the development of *Arabidopsis thaliana*. *Journal of Experimental Botany*, *63*(1), 59–67. https://doi.org/10.1093/jxb/err271

Feijó, J. A., Sainhas, J., Hackett, G. R., Kunkel, J. G., & Hepler, P. K. (1999). Growing pollen tubes possess a constitutive alkaline band in the clear zone and a growth-dependent acidic tip. *Journal of Cell Biology*, *144*(3), 483–496. https://doi.org/10.1083/jcb.144.3.483

Hebenstreit, D., Fang, M., Gu, M., Charoensawan, V., van Oudenaarden, A., & Teichmann, S. A. (2011). RNA sequencing reveals two major classes of gene expression levels in metazoan cells. *Molecular Systems Biology*, *7*(1), 497. https://doi.org/10.1038/msb.2011.28

Hedhly, A., Hormaza, J. I., & Herrero, M. (2009). Global warming and sexual plant reproduction. *Trends in Plant Science*, *14*(1), 30–36.

Hepler, P. K., Rounds, C. M., & Winship, L. J. (2013). Control of cell wall extensibility during pollen tube growth. *Molecular Plant*, *6*(4), 998–1017. https://doi.org/10.1093/mp/sst103

Hepler, P. K., & Winship, L. J. (2015). The pollen tube clear zone: Clues to the mechanism of polarized growth. *Journal of Integrative Plant Biology*, *57*(1), 79–92. https://doi.org/10.1111/jipb.12315

Herrero, M. P., & Johnson, R. R. (1980). High temperature stress and pollen viability of maize. *Crop Science*, *20*(6), 796–800. https://doi.org/10.2135/cropsci1980.0011183X002000060030x

Hofmann, F., Schon, M. A., & Nodine, M. D. (2019). The embryonic transcriptome of *Arabidopsis thaliana*. *Plant Reproduction*, *32*(1), 77–91. https://doi.org/10.1007/s00497-018-00357-2

Honys, D., & Twell, D. (2004). Transcriptome analysis of haploid male gametophyte development in Arabidopsis. *Genome Biology*, *5*(11), R85. https://doi.org/10.1186/gb-2004-5-11-r85

Hsu, P. Y., Calviello, L., Wu, H.-Y. L., Li, F.-W., Rothfels, C. J., Ohler, U., & Benfey, P. N. (2016). Super-resolution ribosome profiling reveals unannotated translation events in Arabidopsis. *Proceedings of the National Academy of Sciences*, *113*(45), E7126–E7135. https://doi.org/10.1073/pnas.1614788113

Huber, W., Carey, V. J., Gentleman, R., Anders, S., Carlson, M., Carvalho, B. S., … Morgan, M. (2015). Orchestrating high-throughput genomic analysis with bioconductor. *Nature Methods*, *12*(2), 115–121. https://doi.org/10.1038/nmeth.3252

Ingolia, N. T. (2016). Ribosome footprint profiling of translation throughout the genome. *Cell*, *165*(1), 22–33.

Ingolia, N. T., Ghaemmaghami, S., Newman, J. R. S., & Weissman, J. S. (2009). Genome-wide analysis in vivo of translation with nucleotide resolution using ribosome profiling. *Science*, *324*(5924), 218–223. https://doi.org/10.1126/science.1168978

Intergovernmental Panel on Climate Change. (2014). *Climate change 2013—The physical science basis: Working Group I contribution to the Fifth Assessment Report of the Intergovernmental Panel on Climate Change*. Cambridge: Cambridge University Press.

Iwata, Y., & Koizumi, N. (2005). An Arabidopsis transcription factor, AtbZIP60, regulates the endoplasmic reticulum stress response in a manner unique to plants. *Proceedings of the National Academy of Sciences of the United States of America*, *102*(14), 5280–5285. https://doi.org/10.1073/pnas.0408941102

Jegadeesan, S., Chaturvedi, P., Ghatak, A., Pressman, E., Meir, S., Faigenboim, A., … Firon, N. (2018). Proteomics of heat-stress and ethylene-mediated thermotolerance mechanisms in tomato pollen grains. *Frontiers in Plant Science*, *9*(1558. https://doi.org/10.3389/fpls.2018.01558

Johnson-Brousseau, S. A., & McCormick, S. (2004). A compendium of methods useful for characterizing Arabidopsis pollen mutants and gametophytically-expressed genes. *The Plant Journal*, *39*(5), 761–775. https://doi.org/10.1111/j.1365-313X.2004.02147.x

Kakani, V. G., Prasad, P. V. V., Craufurd, P. Q., & Wheeler, T. R. (2002). Response of in vitro pollen germination and pollen tube growth of groundnut (*Arachis hypogaea* L.) genotypes to temperature. *Plant, Cell & Environment*, *25*(12), 1651–1661. https://doi.org/10.1046/j.1365-3040.2002.00943.x

Kakani, V. G., Reddy, K. R., Koti, S., Wallace, T. P., Prasad, P. V. V., Reddy, V. R., & Zhao, D. (2005). Differences in in vitro pollen germination and pollen tube growth of cotton cultivars in response to high temperature. *Annals of Botany*, *96*(1), 59–67. https://doi.org/10.1093/aob/mci149

Kandasamy, M. K., & Kristen, U. (1989). Ultrastructural responses of tobacco pollen tubes to heat shock. *Protoplasma*, *153*(1–2), 104–110. https://doi.org/10.1007/bf01322470

Keller, M., Bokszczanin, K. L., Bostan, H., Bovy, A., Chaturvedi, P., Chen, Y., … Consortium, S.-I. (2018). The coupling of transcriptome and proteome adaptation during development and heat stress response of tomato pollen. *BMC Genomics*, *19*(1), 447. https://doi.org/10.1186/s12864-018-4824-5

Kim, D., Paggi, J. M., Park, C., Bennett, C., & Salzberg, S. L. (2019). Graph-based genome alignment and genotyping with HISAT2 and HISAT-genotype. *Nature Biotechnology*, *37*(8), 907–915. https://doi.org/10.1038/s41587-019-0201-4

13653040, 2021, 7, Downloaded from https://onlinelibrary.wiley.com/doi/10.1111/pce.13972 by Bilecik Seyh Edebali, Wiley Online Library on [17/12/2025]. See the Terms and Conditions (https://onlinelibrary.wiley.com/terms-and-conditions) on Wiley Online Library for rules of use; OA articles are governed by the applicable Creative Commons License

Langmead, B., & Salzberg, S. L. (2012). Fast gapped-read alignment with Bowtie 2. *Nature Methods*, *9*(4), 357–359. https://doi.org/10.1038/nmeth.1923

Ledesma, N., & Sugiyama, N. (2005). Pollen quality and performance in strawberry plants exposed to high-temperature stress. *Journal of the American Society for Horticultural Science*, *130*(3), 341–347.

Li, B., Ruotti, V., Stewart, R. M., Thomson, J. A., & Dewey, C. N. (2010). RNA-Seq gene expression estimation with read mapping uncertainty. *Bioinformatics*, *26*(4), 493–500. https://doi.org/10.1093/bioinformatics/btp692

Li, H., Handsaker, B., Wysoker, A., Fennell, T., Ruan, J., Homer, N., … Subgroup, G. P. D. P. (2009). The sequence alignment/map format and SAMtools. *Bioinformatics*, *25*(16), 2078–2079. https://doi.org/10.1093/bioinformatics/btp352

Lin, S.-Y., Chen, P.-W., Chuang, M.-H., Juntawong, P., Bailey-Serres, J., & Jauh, G.-Y. (2014). Profiling of translatomes of in vivo—Grown pollen tubes reveals genes with roles in micropylar guidance during pollination in Arabidopsis. *The Plant Cell*, *26*(2), 602–618. https://doi.org/10.1105/tpc.113.121335

Loraine, A. E., McCormick, S., Estrada, A., Patel, K., & Qin, P. (2013). RNA-Seq of Arabidopsis pollen uncovers novel transcription and alternative splicing. *Plant Physiology*, *162*(2), 1092–1109. https://doi.org/10.1104/pp.112.211441

Lord, E. M., & Russell, S. D. (2002). The mechanisms of pollination and fertilization in plants. *Annual Review of Cell and Developmental Biology*, *18*(1), 81–105. https://doi.org/10.1146/annurev.cellbio.18.012502.083438

Lu, Y., Chanroj, S., Zulkifli, L., Johnson, M. A., Uozumi, N., Cheung, A., & Sze, H. (2011). Pollen tubes lacking a pair of K+Transporters fail to target ovules in Arabidopsis. *The Plant Cell*, *23*(1), 81–93. https://doi.org/10.1105/tpc.110.080499

Mächler, M., Rousseeuw, P., Struyf, A., Hubert, M., & Hornik, K. (2012). *Cluster: Cluster analysis basics and extensions* (Vol. 1). https://cran.r-project.org/web/packages/cluster/.

Maier, T., Güell, M., & Serrano, L. (2009). Correlation of mRNA and protein in complex biological samples. *FEBS Letters*, *583*(24), 3966–3973.

Mallona, I., Weiss, J., & Egea-Cortines, M. (2011). pcrEfficiency: A web tool for PCR amplification efficiency prediction. *BMC Bioinformatics*, *12*(1), 404.

Martin, M. (2011). Cutadapt removes adapter sequences from high-throughput sequencing reads. *EMBnet Journal*, *17*(1), 10–12. https://doi.org/10.14806/ej.17.1.200

Mascarenhas, J. P. (1993). Molecular mechanisms of pollen tube growth and differentiation. *The Plant Cell*, *5*(10), 1303–1314. https://doi.org/10.1105/tpc.5.10.1303

Meijering, E., Jacob, M., Sarria, J.-C. F., Steiner, P., Hirling, H., & Unser, M. (2004). Design and validation of a tool for neurite tracing and analysis in fluorescence microscopy images. *Cytometry, Part A*, *58A*(2), 167–176. https://doi.org/10.1002/cyto.a.20022

Michard, E., Simon, A. A., Tavares, B., Wudick, M. M., & Feijó, J. A. (2017). Signaling with ions: The keystone for apical cell growth and morphogenesis in pollen tubes. *Plant Physiology*, *173*(1), 91–111. https://doi.org/10.1104/pp.16.01561

Müllner, D. (2013). Fastcluster: Fast hierarchical, agglomerative clustering routines for R and Python. *Journal of Statistical Software*, *53*(9), 18. https://doi.org/10.18637/jss.v053.i09

Neukom, R., Steiger, N., Gómez-Navarro, J. J., Wang, J., & Werner, J. P. (2019). No evidence for globally coherent warm and cold periods over the preindustrial Common Era. *Nature*, *571*(7766), 550–554. https://doi.org/10.1038/s41586-019-1401-2

Ohama, N., Kusakabe, K., Mizoi, J., Zhao, H., Kidokoro, S., Koizumi, S., … Yamaguchi-Shinozaki, K. (2016). The transcriptional cascade in the heat stress response of Arabidopsis is strictly regulated at the level of transcription factor expression. *The Plant Cell*, *28*(1), 181–201. https://doi.org/10.1105/tpc.15.00435

Oliveros, J. C. (2015). *Venny. An interactive tool for comparing lists with Venn's diagrams*. Retrieved from https://bioinfogp.cnb.csic.es/tools/venny/index.html

Perez, D. E., Hoyer, J. S., Johnson, A. I., Moody, Z. R., Lopez, J., & Kaplinsky, N. J. (2009). BOBBER1 is a noncanonical Arabidopsis small heat shock protein required for both development and thermotolerance. *Plant Physiology*, *151*(1), 241–252. https://doi.org/10.1104/pp.109.142125

Pina, C., Pinto, F., Feijó, J. A., & Becker, J. D. (2005). Gene family analysis of the Arabidopsis pollen transcriptome reveals biological implications for cell growth, division control, and gene expression regulation. *Plant Physiology*, *138*(2), 744–756. https://doi.org/10.1104/pp.104.057935

Qin, Y., Leydon, A. R., Manziello, A., Pandey, R., Mount, D., Denic, S., … Palanivelu, R. (2009). Penetration of the stigma and style elicits a novel transcriptome in pollen tubes, pointing to genes critical for growth in a pistil. *PLoS Genetics*, *5*(8), e1000621.

Ramírez, F., Ryan, D. P., Grüning, B., Bhardwaj, V., Kilpert, F., Richter, A. S., … Manke, T. (2016). deepTools2: A next generation web server for deep-sequencing data analysis. *Nucleic Acids Research*, *44*(W1), W160–W165. https://doi.org/10.1093/nar/gkw257

Raudvere, U., Kolberg, L., Kuzmin, I., Arak, T., Adler, P., Peterson, H., & Vilo, J. (2019). g:Profiler: A web server for functional enrichment analysis and conversions of gene lists (2019 update). *Nucleic Acids Research*, *47*(W1), W191–W198. https://doi.org/10.1093/nar/gkz369

Reuter, J. A., Spacek, D. V., & Snyder, M. P. (2015). High-throughput sequencing technologies. *Molecular Cell*, *58*(4), 586–597.

Rieu, I., Twell, D., & Firon, N. (2017). Pollen development at high temperature: From acclimation to collapse. *Plant Physiology*, *173*(4), 1967–1976. https://doi.org/10.1104/pp.16.01644

Robinson, J. T., Thorvaldsdóttir, H., Winckler, W., Guttman, M., Lander, E. S., Getz, G., & Mesirov, J. P. (2011). Integrative genomics viewer. *Nature Biotechnology*, *29*(1), 24–26. https://doi.org/10.1038/nbt.1754

Rosenzweig, C., Elliott, J., Deryng, D., Ruane, A. C., Müller, C., Arneth, A., … Jones, J. W. (2014). Assessing agricultural risks of climate change in the 21st century in a global gridded crop model intercomparison. *Proceedings of the National Academy of Sciences*, *111*(9), 3268–3273. https://doi.org/10.1073/pnas.1222463110

Rottmann, T., Fritz, C., Sauer, N., & Stadler, R. (2018a). Glucose uptake via STP transporters inhibits in vitro pollen tube growth in a HEXOKINASE1-dependent manner in *Arabidopsis thaliana*. *The Plant Cell*, *30*(9), 2057–2081. https://doi.org/10.1105/tpc.18.00356

Rottmann, T. M., Fritz, C., Lauter, A., Schneider, S., Fischer, C., Danzberger, N., … Stadler, R. (2018b). Protoplast-esculin assay as a new method to assay plant sucrose transporters: Characterization of AtSUC6 and AtSUC7 sucrose uptake activity in Arabidopsis Col-0 Ecotype. *Frontiers in Plant Science*, *9*(430). https://doi.org/10.3389/fpls.2018.00430

Rutley, N., & Twell, D. (2015). A decade of pollen transcriptomics. *Plant Reproduction*, *28*(2), 73–89. https://doi.org/10.1007/s00497-015-0261-7

Sato, S., Peet, M. M., & Thomas, J. F. (2002). Determining critical pre- and post-anthesis periods and physiological processes in *Lycopersicon esculentum* Mill. exposed to moderately elevated temperatures. *Journal of Experimental Botany*, *53*(371), 1187–1195. https://doi.org/10.1093/jexbot/53.371.1187

Sauer, N. (2007). Molecular physiology of higher plant sucrose transporters. *FEBS Letters*, *581*(12), 2309–2317. https://doi.org/10.1016/j.febslet.2007.03.048

Sauer, N., Ludwig, A., Knoblauch, A., Rothe, P., Gahrtz, M., & Klebl, F. (2004). AtSUC8 and AtSUC9 encode functional sucrose transporters, but the closely related AtSUC6 and AtSUC7 genes encode aberrant proteins in different Arabidopsis ecotypes. *The Plant Journal*, *40*(1), 120–130. https://doi.org/10.1111/j.1365-313X.2004.02196.x

Scarpin, M. R., Sigaut, L., Temprana, S. G., Boccaccio, G. L., Pietrasanta, L. I., & Muschietti, J. P. (2017). Two Arabidopsis late pollen

13653040, 2021, 7, Downloaded from https://onlinelibrary.wiley.com/doi/10.1111/pce.13972 by Bilecik Seyh Edebali, Wiley Online Library on [17/12/2025]. See the Terms and Conditions (https://onlinelibrary.wiley.com/terms-and-conditions) on Wiley Online Library for rules of use; OA articles are governed by the applicable Creative Commons License

transcripts are detected in cytoplasmic granules. *Plant Direct*, *1*(4), e00012. https://doi.org/10.1002/pld3.12

Scharf, K. D., Siddique, M., & Vierling, E. (2001). The expanding family of *Arabidopsis thaliana* small heat stress proteins and a new family of proteins containing alpha-crystallin domains (Acd proteins). *Cell Stress & Chaperones*, *6*(3), 225–237. https://doi.org/10.1379/1466-1268(2001)006<0225:tefoat>2.0.co;2

Schindelin, J., Arganda-Carreras, I., Frise, E., Kaynig, V., Longair, M., Pietzsch, T., … Cardona, A. (2012). Fiji: An open-source platform for biological-image analysis. *Nature Methods*, *9*(7), 676–682.

Storey, J. D., Bass, A. J., Dabney, A., & Robinson, D. (2019). *qvalue: Q-value estimation for false discovery rate control. R package version 2.18.0*. http://github.com/jdstorey/qvalue.

Sugio, A., Dreos, R., Aparicio, F., & Maule, A. J. (2009). The cytosolic protein response as a subcomponent of the wider heat shock response in Arabidopsis. *The Plant Cell*, *21*(2), 642–654. https://doi.org/10.1105/tpc.108.062596

Sze, H., Padmanaban, S., Cellier, F., Honys, D., Cheng, N.-H., Bock, K. W., … Hirschi, K. D. (2004). Expression patterns of a novel AtCHX gene family highlight potential roles in osmotic adjustment and K+ Homeostasis in pollen development. *Plant Physiology*, *136*(1), 2532–2547. https://doi.org/10.1104/pp.104.046003

TeamRStudio. (2019). *RStudio: Integrated development for R*. Retrieved from http://www.rstudio.com/.

Umate, P. (2010). Genome-wide analysis of the family of light-harvesting chlorophyll a/b-binding proteins in Arabidopsis and rice. *Plant Signaling & Behavior*, *5*(12), 1537–1542. https://doi.org/10.4161/psb.5.12.13410

Vermeulen, S. J., Campbell, B. M., & Ingram, J. S. I. (2012). Climate change and food systems. *Annual Review of Environment and Resources*, *37*(1), 195–222. https://doi.org/10.1146/annurev-environ-020411-130608

Vogel, C., & Marcotte, E. M. (2012). Insights into the regulation of protein abundance from proteomic and transcriptomic analyses. *Nature Reviews Genetics*, *13*(4), 227–232.

Wagner, G. P., Kin, K., & Lynch, V. J. (2012). Measurement of mRNA abundance using RNA-seq data: RPKM measure is inconsistent among samples. *Theory in Biosciences*, *131*(4), 281–285. https://doi.org/10.1007/s12064-012-0162-3

Wang, Y., Zhang, W.-Z., Song, L.-F., Zou, J.-J., Su, Z., & Wu, W.-H. (2008). Transcriptome analyses show changes in gene expression to accompany pollen germination and tube growth in Arabidopsis. *Plant Physiology*, *148*(3), 1201–1211. https://doi.org/10.1104/pp.108.126375

Waters, E. R. (2012). The evolution, function, structure, and expression of the plant sHSPs. *Journal of Experimental Botany*, *64*(2), 391–403. https://doi.org/10.1093/jxb/ers355

Xiao, Z., Zou, Q., Liu, Y., & Yang, X. (2016). Genome-wide assessment of differential translations with ribosome profiling data. *Nature Communications*, *7*, 11194. https://doi.org/10.1038/ncomms11194

Xu, Z., Hu, L., Shi, B., Geng, S., Xu, L., Wang, D., & Lu, Z. J. (2018). Ribosome elongating footprints denoised by wavelet transform comprehensively characterize dynamic cellular translation events. *Nucleic Acids Research*, *46*(18), e109–e109. https://doi.org/10.1093/nar/gky533

Zinn, K. E., Tunc-Ozdemir, M., & Harper, J. F. (2010). Temperature stress and plant sexual reproduction: Uncovering the weakest links. *Journal of Experimental Botany*, *61*(7), 1959–1968. https://doi.org/10.1093/jxb/erq053

SUPPORTING INFORMATION

Additional supporting information may be found online in the Supporting Information section at the end of this article.

How to cite this article: Poidevin L, Forment J, Unal D, Ferrando A. Transcriptome and translatome changes in germinated pollen under heat stress uncover roles of transporter genes involved in pollen tube growth. *Plant Cell Environ*. 2021;44:2167–2184. https://doi.org/10.1111/pce.13972

13653040, 2021, 7, Downloaded from https://onlinelibrary.wiley.com/doi/10.1111/pce.13972 by Bilecik Seyh Edebali, Wiley Online Library on [17/12/2025]. See the Terms and Conditions (https://onlinelibrary.wiley.com/terms-and-conditions) on Wiley Online Library for rules of use; OA articles are governed by the applicable Creative Commons License